Atmos. Chem. Phys. Discuss., 5, 6127–6184, 2005
www.atmos-chem-phys.org/acpd/5/6127/
SRef-ID: 1680-7375/acpd/2005-5-6127
European Geosciences Union

Atmospheric Chemistry and Physics Discussions

Case studies of ozone transport between North America and Europe in summer 2000

G. Guerova[1], I. Bey[1], J.-L. Attié[2], and R. V. Martin[3,4]

[1]Laboratoire de Modélisation de la Chimie Atmosphérique, École Polytechnique Fédérale de Lausanne (EPFL), Lausanne, Switzerland
[2]Laboratoire d'Aérologie, Observatoire Midi Pyrénées, Toulouse, France
[3]Department of Physics and Atmospheric Science, Dalhousie University, Halifax, NS, B3H 3J5, Canada
[4]Harvard-Smithsonian Center for Astrophysics, Cambridge, Massachusetts, USA

Received: 30 June 2005 – Accepted: 22 July 2005 – Published: 17 August 2005

Correspondence to: G. Guerova (guergana.guerova@epfl.ch)

Abstract

This paper reports on Long Range Transport (LRT) of ozone and related species over the North Atlantic ocean and its impact on Europe. Measurements of NO_2 and O_3 columns from the GOME and MOPITT satellite instruments are first used in conjunction with the GEOS-CHEM global model of transport and tropospheric chemistry to identify the major events of LRT that reach Europe over the course of the summer 2000. Model simulations are then used to examine surface O_3 observations at a European mountain site and O_3 vertical profiles over several European cities to quantify the impact of the LRT events on the European ozone distributions. Over the course of summer 2000, we identified nine major episodes of pollution transport between North America and Europe, which are in majority associated with WCB/post-frontal outflow (7 events) and zonal transport (2 events). We find that on average three episodes occur per month with the strongest ones being in June. The number and frequency of LRT events that reach Europe after leaving North America is strongly driven by the position and strength of the Azores anticyclone. After leaving North America, the plumes can either i) travel in the North American cyclones, mostly in the Warm Conveyor Belt (WCB), tracking poleward and thus reach Europe at high latitudes; ii) be transported zonally between 40° and 55° N directly to Europe; iii) be incorporated into the Azores anticyclone and reach Europe at mid-latitudes. Based on model sensitivity simulation it can be concluded that on average the North American sources of ozone contribute between 2–8 ppb in PBL and 10–13 ppb in FT. During particular episodes the North American sources resulted in O_3 enhancement up to 25–28 ppb in the layer between 800–600 hPa and 10–12 ppb in PBL. For some episodes a substantial North American contribution (30% or higher) does not translate into a well marked enhancement of the total O_3.

ACPD

5, 6127–6184, 2005

1. Introduction

The long range transport (LRT) of pollution in the Northern Hemisphere is of major importance as the main anthropogenic sources are the populated regions of North America, Europe and in the last decade, Asia. The LRT between North America, Europe and Asia occurs at all altitudes of the troposphere and is a subject of intense observation and modeling efforts. In particular, tropospheric ozone (O_3) has a lifetime of several days, which makes it very suitable to be transported over long distances. The LRT between North America and Europe is currently rising a lot of interest as it has been suggested that North America has a substantial impact on the atmosphere above Europe (e.g., Stohl and Trickl, 1999; Stohl et al., 2002; Li et al., 2002; Auvray and Bey, 2005). For example, 11% of the tropospheric ozone burden over Europe in summer is found to be due to precursors emitted over North America, while the European sources are responsible for only 10% (Auvray and Bey, 2005). In this paper, we use a three-dimensional global model of chemistry and transport simultaneously with several observational datasets to quantify the impact of individual LRT events on O_3 distributions over Europe.

The LRT of O_3 between North America and Europe has significant seasonal variations. The O_3 flux due to precursors emitted over North America, has a maximum in spring and summer due to increased photochemical activity and favorable weather patterns (Auvray and Bey, 2005). Li et al. (2005a) recently investigated the predominant pathways of North American pollution export to the North Atlantic Ocean in summer. They found that export from North America is controlled by the fast-moving mid-latitude cyclones tracking eastward across North America. Cyclogenesis over continental US occurs predominantly at two locations, i) at the lee side of the Rocky Mountains (4 events per month in summer 2000), and ii) over the east coast of US (3 events during summer 2000). Li et al. (2005a) also reported one event of pollution export associated with a east-west stationary front that induces a strong zonal outflow. The pollution is predominantly exported in the latitude range between 30 and 55° N through these cy-

ACPD
5, 6127–6184, 2005

clones, but a few events of high-latitude outflow associated with high-latitude cyclones are also found (5 in the course of summer 2000) (Li et al., 2005a). In general, pollutants are lifted outside of the boundary layer at pressure levels 700 to 500 hPa ahead of the cold fronts associated with the cyclones in the Warm Conveyor Belt (WCB) (Stohl, 2001). Strong outflow is also found behind the cold fronts at low altitudes. In average, the carbon monoxide (CO) flux exported out off North America is reported to be 50% larger at altitudes below 3 km. Finally, deep convection, especially over southeastern and central US also contributes to the ventilation of the boundary layer (Li et al., 2005a; Auvray and Bey, 2005).

We build on the work of Li et al. (2005a) to examine further the North American outflow and to quantify its impact on Europe. We first use satellite retrievals of CO and nitrogen dioxide (NO_2) in combination with the GEOS-CHEM model to identify the major events of LRT that enter Europe during the summer 2000. The MOPITT CO observations offer a good signature of continental outflow, while the GOME NO_2 observations provide an additional indication of chemical environment in the plumes (Li et al., 2005a; Choi et al., 2005). We then use the model to examine O_3 concentrations at the mountain site Jungfraujoch (3580 m a.s.l., Switzerland) as well as ozone vertical profiles provided by the Measurement of Ozone and Water Vapor by Airbus In-Service Aircraft (MOZAIC) program, to quantify the impact of LRT events on O_3 distributions over Europe. The Jungfraujoch station presents the advantage to be located in the center of Europe and in the Free Troposphere (FT) and is, thus, susceptible to be a receptor point for most of LRT events. The MOZAIC profiles allow examination of LRT events throughout the troposphere with good temporal and spatial resolution.

This paper is organized as follows. Section 2 presents the different datasets used, i.e. satellite retrievals of CO and NO_2 from the MOPITT and GOME instruments, respectively, the ground based observations at the Jungfraujoch and the MOZAIC vertical profiles. The GEOS-CHEM model used in this work is described in Sect. 3 of the manuscript. The atmospheric circulation and detailed description of the LRT episodes entering Europe are presented in Sect. 4. The impact of North American plumes on

O_3 distributions in Europe is examined in Sect. 5. Conclusions are given in Sect. 6.

2. Observation datasets

2.1. Carbon monoxide retrievals from MOPITT instrument

The MOPITT instrument flies on the NASA EOS Terra satellite which has a near-polar, sun-synchronous orbit with an inclination of approximately 98.2 degrees with respect to the equator, an altitude of 705 km, a descending node crossing time 10:30 LT and a global coverage in approximately three days. MOPITT is a nadir sounding instrument with field-of-view 22×22 km^2 (http://www.atmosp.physics.utoronto.ca/MOPITT/mdd_93/index.html). The field of view is continuously scanned through a swath of about 600 km wide thus increasing the spatial coverage. A detailed description of the MOPITT-CO retrieval algorithm can be found in Deeter et al. (2003). The measured radiances are inverted to CO profiles using an optimal estimation algorithm and a radiative transfer model described in Edwards et al. (1999). Retrievals of CO may involve up to twelve measured signals in the two measurement bands. Only clear-sky radiances, i.e., uncontaminated by clouds, are fed to the retrieval algorithm.

The MOPITT Version 3 data are available for the period March 2000–May 2001. The daytime and nighttime CO profiles are retrieved on seven pressure levels: surface, 850, 700, 500, 350, 250, 150 hPa and correspond to the global measurements between 65° S and 65° N. The maximum likelihood retrieval algorithm used in the MOPITT data processing incorporates a priori information into the retrieval. This is a must in the radiances processing due to the non-uniqueness of the solution. For a detailed description of computation of the averaging kernel matrix we refer to: 'Calculation and Application of MOPITT Averaging Kernels' (PDF, by M. Deeter, updated 24 July 2002, available at: http://www.eos.ucar.edu/mopitt/data/index.html). For the comparison with GEOS-CHEM the MOPITT observations have been averaged over the 2×2.5°model grid. In addition the GEOS-CHEM CO has been transformed applying the MOPITT av-

ACPD
5, 6127–6184, 2005

eraging kernel matrix. Similarly to Heald et al. (2003) the averaging kernels are applied to the GEOS-CHEM CO column.

2.2. Nitrogen dioxide retrievals from GOME

The GOME instrument was launched on board of the European Space Agency ERS-2 satellite in April 1995. The satellite has a sun-synchronous polar orbit with an inclination of 98° with respect to the equator, a mean altitude of 780 km, equator crossing at 10:30 LT and a global coverage in approximately 3 days. GOME has a nadir-scanning ultraviolet and visible spectrometer for global monitoring of total atmospheric ozone and nitrogen dioxide (Burrows et al., 1999). The instrument has a field-of-view of $320\times40\,km^2$ ($2.8°\times0.14°$). Satellite observations of tropospheric constituents are much more difficult than for the stratosphere due to interferences with clouds and aerosols, inhomogeneities in the ground albedo and the stratospheric contributions. In the retrieval of NO_2 from GOME those contributions have been taken into account.

Our version 2 retrieval of tropospheric NO2 columns from GOME is based on the version 1 algorithm described in(Martin et al., 2002) with the following differences. The slant NO_2 columns are obtained by nonlinear least-squares fitting of in the 426–452 nm spectral region. All interfering species are fitted in this spectral window. The H_2O-ring effect is no longer included as an interfering species. A 241°K NO_2 spectrum (Burrows et al., 1998) is used in the retrieval. Following Richter and Burrows (2002), a single solar reference spectrum, specifically 11 June 2000, is used to eliminate the daily varying bias caused by the diffuser plate on the GOME instrument (Richter and Wagner, personal communication, 2001; Martin et al., 2002). The most pronounced difference between the version 1 and version 2 tropospheric NO_2 columns occurs over deserts where the version 2 data are lower by about 5×10^{14} molec cm^{-2}. The details of the subsequent processing are described in Martin et al. (2002) and Martin et al. (2003). Briefly, the stratospheric component is computed over the remote Pacific Ocean and subtracted to obtain the tropospheric slant columns. The tropospheric slant columns are converted to vertical columns using an Air Mass Factor (AMF). The AMF is calcu-

ACPD
5, 6127–6184, 2005

lated from the integral of the relative vertical NO_2 distribution from the GEOS-CHEM weighted by altitude-dependent scattering weights (Palmer et al., 2001), computed with the LIDORT (Spurr, 2002) radiative transfer model. The temperature dependence of the NO_2 cross-section is accounted for in the AMF calculation. Clouds scattering is accounted for using local cloud information determined from GOME (Kurosu et al., 1999). It should be mentioned that GOME is almost twice as sensitive to tropospheric NO_2 columns over ocean than over land. Clouds enhance the sensitivity of GOME to NO_2 columns over ocean, increasing the AMF by up to 40% with respect to clear-sky. Over continental regions with high surface emissions, the AMF is typically 20–30% lower than clear-sky AMFs due to the obscuration of boundary layer NO_2 by clouds. We exclude scenes in which the cloud radiance fraction exceeds 50% to reduce the retrieval uncertainty. The typical uncertainty estimate for each observation is ± (1×10^{15} molec cm^{-2} + 40%). After accounting for random errors, the monthly-mean uncertainty reduces to ± (5×10^{14} molec cm^{-2} + 30%).

2.3. Surface observations of O_3 at the Jungfraujoch

O_3 measurements at the Jungfraujoch (JFJ) are performed with a UV absorption instrument. Estimated standard uncertainty for hourly averages is 1.2 ppb for values below 60 ppb and 2% for values greater than 60 ppb. The JFJ site is at an altitude of 3580 m a.s.l. (650 hPa) and is surrounded by industrialized regions. The JFJ is predominantly situated in the free troposphere (57% of the time according to Li et al., 2005b[1]), but convection or frontal intrusions frequently bring planetary boundary layer air to the site (Baltensperger et al., 1997; Zellweger et al., 2003) especially during the warmer months. The wind direction at the site is influenced by the NE-SW orientation of the local alpine watershed in the immediate vicinity, resulting in an average annual wind

[1]Li, Y., Staehelin, J., Auvray, M., Bey, I., and Schultz, M.: Comparison between numerical simulations of two 3-D global models (GEOS-CHEM and MOZART) with ozone observations at Jungfraujoch (Switzerland) and ozone sondes from Payerne, Atmos. Environ., submitted, 2005b.

frequency of 60% from north-west and 30% from south-east according to MeteoSwiss (Baltensperger et al., 1997).

2.4. O_3 vertical profiles from MOZAIC

MOZAIC O_3 concentrations are measured on board of commercial aircraft by a dual beam UV absorption instrument. The overall precision of the data is ± (2 ppb + 2%). O_3 measurements have been validated using ozonesonde data. In the free troposphere (800–300 hPa) the agreement found (3 to 13%) was well within the uncertainty of the two techniques (Thouret et al., 1998). In this manuscript we used MOZAIC profiles over Brussels, Paris and Frankfurt airports. On average two profiles per day are available at each airport. For the comparison with GEOS-CHEM, the observations are interpolated to the model pressure levels.

3. Global Chemistry Transport Model: GEOS-CHEM

3.1. Model description and simulation

In this manuscript, we used the GEOS-CHEM model, version 5-07-08 with an horizontal resolution of 2° of latitude by 2.5° of longitude and 30 vertical levels from the surface to 0.01 hPa with 18 levels in the troposphere (http://www.as.harvard.edu/chemistry/trop/geos). A brief description of the model is given below. Further details can be found in Bey et al. (2001), Martin et al. (2003) and Park et al. (2004).

The model is driven by meteorological fields provided by the Global Circulation Model GEOS-3 of the Global Modeling and Assimilation Office (GMAO) at NASA with a temporal resolution of 3 and 6 h. 31 tracers are transported to provide a comprehensive description of the NO_x-O_x-VOC chemistry and nitrate-ammonium-sulphate aerosol chemistry. A total of 300 chemical reactions are taken into account in the chemical mechanism for about 80 different species, as described in Fiore et al. (2003). The photolysis

ACPD
5, 6127–6184, 2005

rates are calculated with the Fast-J algorithm (Wild et al., 2000), which accounts for clouds and aerosols. When not provided by the model itself, aerosols are taken from the GOCART model (Chin et al., 2002) and coupled to the GEOS-MODEL model as described in Martin et al. (2003). The dry deposition velocities are computed using a resistance-in-series model described in Wesely (1989) and modified by Wang et al. (1998a). Wet deposition is applied to aerosols, HNO_3 and H_2O_2 as described in Liu et al. (2001).

Anthropogenic emissions of NO_x, CO and NMCs are prescribed as monthly mean fluxes. They are derived from extensive compilations of energy use and combustion efficiency data (Wang et al., 1998b) and further scaled to the year 2000 as described in Bey et al. (2001). Natural emissions from plants and NO_x sources from lightning are calculated on-line with different parameterizations in order to capture their large variability. Biomass burning emissions are included on monthly bases and are specified for 2000 using Aerosol Index (AI) data from TOMS as well as ATSR (Along Track Scanning Radiometer) observations as described in Duncan et al. (2003).

In the transport algorithm the three-dimensional continuity equation is solved using a flux-form semi-Lagrangian method (Lin and Rood, 1996). The basic constraint is a mass conservation as well as consistency of the flow and stability. Moist convection is parameterized as formulated in Allen et al. (1996a) and Allen et al. (1996b). Assumed is a full mixing within the boundary layer extent, which is specified based on meteorological fields.

In this study, results are shown from a standard simulation for 2000 obtained after a one-year spin up. A sensitivity simulation was also conducted in which anthropogenic emissions from North America are turned off. The subtraction of these results from that of the standard simulation allows quantification of the fraction of O_3 only due to North American sources (further referred to as North American O_3). Tagged O_3 simulation is performed to separate the stratospheric contribution. In that simulation, the production and loss rates archived from the standard simulation are used to drive an off-line simulation, in which different O_3 tracers are transported and tagged according to their

region of production.

3.2. Model evaluation

The model has been previously the subject of several global evaluations (e.g., Bey et al., 2001; Martin et al., 2003). Regional validations were presented by Fiore et al. (2002) and Li et al. (2005a) for the United States, Li et al. (2002) for the Western North Atlantic Ocean, and Duncan and Bey (2004) and Auvray and Bey (2005) for Europe. Evaluation of O_3 and CO on a global scale does not show obvious biases. However, monthly means O_3 show a too low seasonal variations especially in the mid-troposphere, i.e., at the 500 hPa level (Bey et al., 2001; Fusco and Logan, 2003). Over Europe, monthly means surface CO was found to be too low in winter and spring by 22 ppb and too high in summer and fall by 20 ppb (Auvray and Bey, 2005).

Figure 1 compares monthly averaged tropospheric CO column from GEOS-CHEM and from MOPITT for June 2000. This month is shown as an example since in 2000, it is the summer month for which LRT episodes are more frequent, and CO concentrations over the North Atlantic are the strongest compared to July and August (not shown). The model overestimates CO columns over Canada, Eastern Europe, and over the North Atlantic, resulting in a positive bias of 7% (Table 1) and correlation of 0.59. The model overestimate, well pronounced in July and August, is believed to be due to too low OH concentrations. We find a global methyl chloroform (CH_3CCl_3) lifetime close to 7 years in this version of the model, while CH_3CCl_3 observations rather suggest a lifetime against tropospheric OH of about 5.5 years (Spivakovsky et al., 2000; Lelieveld et al., 2004). The reason for these too low OH concentrations is unclear at this moment, but may reflect a problem in the model associated with cloud optical depths.

The comparison between monthly mean NO_2 from GEOS-CHEM and from GOME for June 2000 is shown in Fig. 2. In contrast to CO the model shows a well pronounced underestimate of NO_2 columns ranging from −32 to −42% for the entire summer and over the region of interest. The correlation 0.81 (Table 1) is however good, indicating a correct representation of the spatial variation of NO_2. Note that Auvray and Bey (2005)

ACPD
5, 6127–6184, 2005

also pointed out that the model underestimates surface NO_2 concentrations by about 17% over Europe especially in summer. Similar results were also reported in a recent global model intercomparison experiment by Dentener et al. (2005)[2]. They found that the averaged model maxima of 6–8 10^{15} molec cm^{-2} is clearly underestimating the GOME observed values, which exceed 10 10^{15} molec cm^{-2}, indicating possible problems with NO_xemissions or other factors such as model chemistry and resolutions.

Figure 3 shows a comparison between monthly mean O_3 profiles as provided by MOZAIC and simulated over Brussels, Paris, Frankfurt, while Table 2 summarizes a number of statistical quantities calculated using individual profiles. Figure 3 shows that the model reproduces in general the observed features of the monthly mean O_3 profiles. However, the model systematically underestimates O_3 in the FT by about 7 ppb (12%) while it overestimates O_3 by about 3 ppb (6%) in the PBL. Observed surface O_3 has to be considered with caution. High concentrations of NO_x close to the airports and in general in the PBL close to large cities induce a strong titration of O_3, which may not be reflected in the model grid. In the FT, the reasons for the model underestimate are unclear, but could reflect problems with the magnitude of the stratospheric flux, the role of European sources (e.g., mixing between PBL and FT) and/or the influence of North American sources.

4. Transport of CO and NO_2 over the North Atlantic

4.1. Airflow patterns over the North Atlantic in summer 2000

Figure 4 presents the model monthly mean winds at 500 hPa in summer 2000. In June 2000 (Fig. 4a), there are two well marked large scale circulation patterns, namely the Azores extratropical anticyclone and the cyclone located between Greenland and Iceland. Between those two distinct systems a strong westerly flow (20 m/s) is well seen

[2]Dentener, F., Stevenson, D., Ellingsen, K., Noije, T., Schultz, M., and Amann, M.: Global air quality for the next generation, J. Geophys. Res., submitted, 2005.

at 500 hPa between 45°–55° N. The circulation in July (Fig. 4b) is mostly driven by the Azores anticyclone, which has expanded to the north and covers almost completely the North Atlantic. A strong southwesterly flow is seen along the east coast of the North America. The Azores anticyclone in August is present only to the south of the North Atlantic. Between 40°–50° N a westerly flow is predominant at the 500 hPa model level (Fig. 4c). The Azores anticyclone is a persistent pattern in summer 2000 over the North Atlantic, and its position and strength are the key parameters that drive the pollution transport from North America to Europe.

In contrast to Li et al. (2005a), the present work focuses on air masses with a North American origin which cross the North Atlantic Ocean and impact Europe. After leaving North America, those air masses can either i) travel in the North American cyclones tracking poleward and thus reach Europe at high latitudes; ii) be transported zonally between 40°and 55° N directly to Europe; iii) be incorporated into the Azores anticyclone and reach Europe or they may travel back towards North America and never reach Europe.

WCB of Atlantic cyclones are efficiently ventilating the east cost of North America, but in the summer time not all WCB reach Europe. When they reach Greenland they can be either dispersed due to occlusion or intercepted in a new WCB during cyclogenesis of an Iceland low. Such an example was reported by Cooper et al. (2004) during the ITCT 2K2 campaign in the North Pacific. In the following, we describe the pathways of a number of long range transported air masses as they leave North America, travel over the North Atlantic and enter Europe. We identify a total of nine LRT events in summer 2000 in both the model and the observations.

4.2. June 2000

According to Li et al. (2005a) the first WCB uplift over North America occurred in the period 4 to 6 June (not shown). On 4 June elevated model CO concentrations are seen along the east coast of North America and Labrador sea. They are associated with a cyclone located over the Gulf of Saint Lawrence moving northeastward toward

Greenland, a typical summertime trajectory (Li et al., 2005a). On the next day the cyclone is stationed south of Greenland and a CO plume can be located in the model at 700 hPa. During the following days the cyclone occludes and the CO is dispersed. This example illustrates one case of North American outflow that does not reach Europe.

The first episode of LRT, with a clear impact on Europe further denoted as LRT1, is presented in Fig. 5. In the period 9–13 June the circulation over the Atlantic can be summarized as follows: i) 8–9 June: development of extratropical anticyclone over the Azores and cyclogenesis in the Hudson Bay, ii) 10–13 June: anticyclone extends toward southern Europe, while the low pressure system moves northeastward toward Greenland. Between those distinct structures westerly-south-westerly winds are prevailing with a wind speed of 20 m/s at 850 hPa and 40 m/s at 500 hPa. In this open channel (Fig. 5e) the anthropogenic emissions from the central Atlantic states of US are directed towards Europe, i.e. the British Isles and Scandinavia. Li et al. (2005a) attribute pollution uplift within the WCB region of a semi-stationary east-west cold front and the subsequent post-frontal transport. This strong episode is clearly seen in the MOPITT CO column (Fig. 5c) despite the observation gaps. NO_2 observations (Fig. 5d) also show an enhancement close to the US coast, where the maximum NO_2 is presented in the shape of a 'tongue'. However, based on the model predictions, it does not clearly reach Europe likely due to the shorter lifetime of NO_2 compared to that of CO.

The LRT2 episode occurred in the period 19–21 June (Fig. 6). A CO plume from the Gulf of Saint Lawrence transported by an Atlantic cyclone moving northeastward is clearly seen in the model at latitude greater than 50° N. While reaching Iceland, the cyclone deepens and moves toward Europe reaching the British Isles on 22 June (Fig. 6e) and continuing toward Norway where it occludes. The CO enhancement could not be confirmed in the MOPITT retrieval (Fig. 6c) because there is an observation gap exactly at the plume location. Updrafts in the WCB sector of cold fronts are associated with cloud formation, but only cloud free pixels are used in MOPITT retrieval. No clear enhancement of NO_2 associated with this LRT2 is seen neither in the GOME

observations nor in the model. It is to be noted that NO_2 enhancement is seen in both the observations and the model more to the south at about 42° N. Sensitivity model simulation indicates that this enhancement is restricted to the lower troposphere and is likely to be associated with post-frontal outflow. The transport is taking place at the periphery of the Azores anticyclone and the plume is then turning anticyclonicly, i.e. to the south, shortly before reaching Europe.

In the period 24 to 26 June, an accumulation of anthropogenic CO of Canadian origin occurs in the Gulf of Saint Lawrence (not shown), facilitated by a stationary cyclone. The cyclone continues toward Europe in the period 27 to 29 June inducing a third major LRT episode (LRT3). The trajectory is however different from the one described in the previous two cases. Because of a blocking anticyclone located over Norway, the cyclone moves southeast and reaches the European coast close to Portugal. The cyclone stay stationary west of France, where it occludes around 3 July.

4.3. July 2000

The fourth episode (LRT4) is observed in the period 7–9 July (Fig. 7). According to Li et al. (2005a) North American pollution is uplifted within the WCB of an Atlantic cyclone located over the Gulf of Saint Lawrence (Fig. 7c). The CO plume is well seen in GEOS-CHEM close to Greenland at 700 hPa on 8 July (Fig. 7a). It travels towards Europe and on 9 July reaches the British Isles. Further the plume is transported by a new cyclone located over the North Sea. NO_2 enhancement is also observed south of Greenland on 8 July (Fig. 7b). At the same time the Azores anticyclone is occupying the entire North Atlantic and thus the transport is taking place at the northern part of the Ocean. During this period the MOPITT and GOME data are not available for intercomparison.

At the time of the LRT4 arrival in Europe, a new cyclogenesis occurs on 7–8 July over the mid-Atlantic east coast of North America (Li et al., 2005a). The cyclone tracks northeastward towards Newfoundland and on 15 July centers over Scandinavia where the occlusion occurs. On 11 July a distinct CO plume associated with the WCB sector of the cyclone is seen in the model at 500 hPa over the Labrador sea (LRT5). The

LRT5 plume has a similar trajectory as LRT4. Due to lack of GOME and MOPITT data the plume can be seen only in the model simulations.

The LRT6 event was associated with aged pollution plume, intercepted by a cyclone and entering Europe through the southwest border, i.e., Portugal and Spain. The cyclone occludes in the period 26–27 July. Both MOPITT and GOME detect enhanced concentrations at the latitude 30–15° W and longitude 40° N on 25–26 July. This enhancement is possibly associated with post-frontal outflow associated with the cold front of the anticyclone.

The seventh major LRT event is associated with WCB outflow of a North American cyclone formed on 24–25 July, which slowly moves towards the Azores and enters Europe from the southwestern border around 30 July similarly to LRT6. The cyclone moves to the northeast and reaches central Europe on 1 August.

4.4. August 2000

The eight event (LRT8) occurs in the period 2–6 August (not shown). North American CO accumulated over Iceland where cyclogenesis occurs on 4 August. Within the newly formed cyclone the North American CO emissions are trapped and further transported towards Europe. The cyclone and the plume reach Scandinavian peninsula on 5 August. The LRT8 occurs to the very northern border of the North Atlantic as the Azores anticyclone spreads to the north covering almost completely the ocean. There is no MOPITT and GOME data available for the region of interest.

A zonal LRT event (LRT9) is observed in the period 10 to 14 August (Fig. 8). Both NO_2 and CO are transported by the strong westerly winds between the cyclone to the north and the Azores anticyclone to the south of the North Atlantic (Fig. 8e). Similarly to the LRT1 episode the transport is observed in the lower troposphere. The outflow and transport are distinct in the GEOS-CHEM at 700 hPa as well as in the MOPITT CO total column. Elevated NO_2 concentrations are also observed in GOME over the North Atlantic at 45° N, but only limited data are available for this period and region.

To summarize, over the course of summer 2000, we identified nine episodes of pol-

lution transport between North America and Europe, which are in majority associated with WCB/post-frontal outflow (7 events) and zonal transport (2 events). We find that on average three episodes occur per month with the strongest one being in June 2000.

5. Impact of LRT events on O_3 distributions over Europe

5.1. O_3 at Jungfraujoch

Figure 9 shows O_3 concentrations observed at JFJ and simulated by GEOS-CHEM in the period June–August 2000, along with the model North American and stratospheric contributions. The model underestimates the observed O_3 concentrations, and captures only some of the temporal variability (r=0.3 over the summer 2000). As mentioned previously, the JFJ site is a mountain site which is frequently impacted by fronts, foehn events and thermal lifting that bring planetary boundary layer air with potentially high O_3 concentrations especially in summer. Even though Li et al. (2005b)[1] find that these events do not contribute much to the monthly mean ozone concentrations, they could have some impact on hourly values. Because of coarse resolutions, these events are difficult to represent in global models (for additional discussion, see Li et al., 2005b[1]). Despite these limitations, we examine the North American O_3 contribution at JFJ. The nine major LRT episodes identified with the model and the MOPITT observations are marked by arrows in Fig. 9. The averaged North American O_3 contribution is 9 ppb in summer 2000. Increases in the North American contribution above this mean value can be attributed to each of the previously discussed LRT event. During those events, the North American ozone at JFJ increases up to 20 ppb, and in some cases the enhancement is seen over several days. Note that the strongest LRT events are not associated with the highest levels in O_3 concentrations, which makes their identification in the O_3 observations difficult.

ACPD
5, 6127–6184, 2005

5.2. O_3 profiles over Brussels, Paris and Frankfurt

In this section, we further examine the impact of North American pollution by comparing individual profiles measured on board of MOZAIC airplanes and simulated by the model over several cities in Europe. In particular, we attempt to analyze O_3 profiles observed during four representative LRT events using the model sensitivity simulations that provide North American and stratospheric O_3 contributions. Although imperfect, numerical models provide the only mechanism to attribute ozone enhancements to LRT from a specific source region. Here we apply the GEOS-CHEM model to interpret the observed MOZAIC profiles of O_3 and quantify the impact of North American plumes on European O_3 distributions.

Impact of the first event LRT1, is illustrated in Fig. 10 as the plume enters the European region on 13 June (Fig. 10a) and expands on 14 June (Fig. 10b). The observed and model O_3 profiles averaged over the three-day episode (Fig. 10c) show very good agreement above 900 hPa. Note, however, that as expected, the variability (expressed by the standard deviation around the mean value) is much greater in the MOZAIC profile compared to GEOS-CHEM. At Brussels, the observed O_3 profiles at 12:00 and 20:00 UTC on 14 June (Fig. 10e) differ from those observed on 13 June and show an increase of about 25 ppb between 500 and 600 hPa and around 750 hPa, respectively. According to the model (Fig. 10d), the increase on 14 June can be attributed to North American O_3 with a maximum of 20 ppb between 850 and 650 hPa. This is in agreement with the observed increase, even though the model does not capture the variability over the course of 14 June. On 15 June, an O_3 enhancement in the range 20–30 ppb is observed at lower altitude (within the boundary layer), but the model attributes only 8 ppb to be due to long range transport from North America. The model stratospheric contribution (Fig. 10d) is low (<10 ppb) during that episode. The LRT1 plume is also intercepted in MOZAIC profiles in Frankfurt and Paris with the North American enhancement at the same altitude as in Brussels (see Fig. 14). We find that the North American O_3 contributes for more than 20 ppb during this episode, which is

ACPD
5, 6127–6184, 2005

the strongest one for summer 2000 according to the model.

The LRT2 plume is approaching the British Isles on 21 June as seen in Fig. 11a. It enters Europe on 22 June and is intercepted over Paris (white dot in Fig. 11b). The comparison between the observed profiles on 21 June and those on 22 and 23 June shows an enhancement of about 15 ppb between 700 and 600 hPa, which is likely associated with North American sources, as diagnosed with the sensitivity model simulations (Fig. 11d). Above 550 hPa an enhancement of about 25 ppb is also observed on 23 June, which is likely associated with stratospheric input (Fig. 11d). However, it should be noted that the model does not correctly reproduce the magnitude of the stratospheric O_3 flux in the layer between 500–300 hPa as indicated by the significantly low model variability compared to the observed one (Fig. 11c). During that episode, the model indicates that the North American O_3 contributes at the most to about 15 ppb. In the lower troposphere the simulated enhancement of North American contribution at 02:00 UTC on 22 June might be overestimated as the model tends to overestimates the observed O_3 concentrations throughout the episode.

The LTR4 plume reaches Europe at high altitude on 8 July and spreads towards central Europe on 9 July as seen in Fig. 12a and b. In general the model profile, averaged over the episode, compares well with the observed one (Fig. 12c). Note however, that below 700 hPa the model exhibits an overestimate of the observed O_3 in the range of 10 ppb, which is within the observed standard deviation. On 8 July (Fig. 12e), the observed and model O_3 concentrations remain constant with height to about 40 ppb, except for a strong increase (greater than 100 ppb) above 550 hPa, which is likely associated with stratospheric input and, to some extent to North American contribution. On 9 June at 14:00 UTC, an O_3 layer of North American origin is observed between 750 and 500 hPa while the O_3 concentrations in the upper troposphere is substantially reduced (less than 40 ppb). By the next day, this layer disappeared, but an increase of stratospheric origin is again seen in the upper troposphere. Over these 3 days, a strong variability is also seen in the boundary layer, where O_3 varies from 2 to 30 ppb. The simulated North American enhancement (Fig. 12d) reaches 20 ppb and

is seen over a large region of the troposphere (from 800 to 500 hPa) on 9 and 10 July.

The arrival of LRT9 plume is illustrated in Fig. 13. As seen in Fig. 13c the model clearly underestimates O_3 concentrations in the mid troposphere. At 10:00 UTC on 13 August, the observed O_3 in the lower troposphere increases compared to 04:00 UTC. However, this is not associated with any LRT as indicated by the model sensitivity simulations (Fig. 13a). This enhancement probably reflects the O_3 diurnal variation associated with local photochemical activity during stagnation period. The observed O_3 concentration below 500 hPa decrease on 14 August in comparison with that observed on 13 August, which is likely reflecting a change in local photochemical activity. Nevertheless the model predicts a substantial contribution of North American O_3 of about 12 to 18 ppb at 700 hPa (Fig. 13d). It should be noted that for this episode, the enhancement is not clearly seen in the MOZAIC profiles (Fig. 13e), except maybe at 800 hPa on 15 August.

A generalization of the approach used to quantify the impact of LRT events on O_3 distribution over Europe is provided in Fig. 14, which shows the simulated North American O_3 contributions at 00:00 UTC and 12:00 UTC for each day of June, July and August 2000 over Brussels, Paris and Frankfurt. The color dots correspond to the episodes discussed in the text and it is clear from Fig. 14 that the strongest episodes have been identified. Based on individual cases, the North American contribution presents a broad maximum between 700 and 400 hPa, and reaches up to 28 ppb in one case. In the boundary layer (i.e. below 800 hPa), the North American contribution rarely exceeds 12 ppb. The monthly mean profiles of North American O_3 over the three selected cities are similar, and increase from about 5 ppb in the boundary layer to about 12 ppb in the middle and upper troposphere. The monthly averaged contribution is larger in June and July than in August. However, it is unclear at the moment whether this is typical of the summertime months or whether this is specific to the year 2000.

ACPD
5, 6127–6184, 2005

6. Summary and conclusions

This paper aims to identify LRT events from North America to Europe using a global model of transport and tropospheric chemistry in conjunction with CO and NO_2 satellite observations provided by the MOPITT and GOME instruments, respectively. The number and frequency of LRT events that reach Europe after leaving North America appear to be strongly driven by the position and strength of the Azores anticyclone. After leaving North America, the plumes can either i) travel in the North American (WCB) cyclones tracking poleward and thus reach Europe at high latitudes; ii) be transported zonally between 40°and 55° N directly to Europe; iii) be incorporated into the Azores anticyclone and reach Europe at mid-latitudes. It should be noted however that not all the plumes that leave North America reach Europe. In some cases, for example if the plumes are transported at the periphery of the Azores high, they may travel back towards North America and never reach Europe. The LRT episodes clearly identified in the model are better seen in the observations in cases of zonal transport (e.g., LRT1) as the satellite retrievals are not possible in the cloud covered regions associated with WCB outflow.

During summer 2000, we identify a total of 9 major LRT events, which are in majority associated with WCB/post-frontal outflow (7 events) and zonal transport (2 events). On average three episodes occur per month with the strongest ones being in June 2000. Their impact on the O_3 distributions over Europe are quantified using O_3 observations at the mountain site of Jungfraujoch and O_3 individual vertical profiles provided by the MOZAIC program over three major European cities. Although the model clearly shows substantial limitations in the representation of individual observed profiles, it is possible to analyze the observed O_3 vertical profiles in light of several model sensitivity simulations that provide the North American O_3 and stratospheric O_3 contributions. As expected, the O_3 profiles reflect a complex mixture of individual processes, including local photochemical activity, stratospheric intrusion and transport from North America. The LRT impact is seen at a very large altitude range and with varying strength over the

ACPD
5, 6127–6184, 2005

course of the summer. Based on model sensitivity simulation it can be concluded that on average the North American sources of ozone contribute between 2–8 ppb in the boundary layer and 10–13 ppb in the middle and upper troposphere. During particular episodes the North American sources can result in O_3 enhancement up to 25–28 ppb in the layer between 800–600 hPa and 10–12 ppb in the boundary layer. We find that a substantial North American contribution (e.g., 30% or higher) does not always translate into a well marked enhancement of the total O_3 (e.g., LRT4 and LRT9). The June and July months appear to be more strongly impacted than August. Further work is needed to investigate to what extent our results are specific to the year 2000.

Our analysis reveals the difficulty of assessing the impact of LRT events on European O_3 distributions based on the sole use of O_3 observations. This study also indicates that a clear assessment of the impact on LRT on a given region can only be achieved through a dense networks of measurement sites that provide vertical profiles with a high temporal resolution.

Acknowledgements. We would like to acknowledge the MOPITT, GOME and MOZAIC teams. The GEOS-CHEM model is managed by the Atmospheric Chemistry Modeling Group at Harvard University with support from the NASA Atmospheric Chemistry Modeling and Analysis Program. We also acknowledge the use of high quality observations at Jungfraujoch provided by the network NABEL and the Swiss Agency of Environment, Forest and Landscape (SAEFL), Bern. We thank S. Reimann (EMPA) for helpful discussion about NABEL data.

References

Allen, D. J., Kasibhatla, P., Thompson, A. M., Rood, R. B., Doddridge, B. G., Pickering, K. E., Hudson, R. D., and Lin, S.-J.: Transport-induced interannual variability of carbon monoxide determined using a chemistry and transport model, J. Geophys. Res., 101(D22), 28 655–28 670, 1996a. 6135

Allen, D. J., Rood, R. B., Thompson, A. M., and Hudson, R. D.: Three-dimensional radon 222 calculations using assimilated meteorological data and a convective mixing algorithm, J. Geophys. Res., 101(D3), 6871–6882, 1996b. 6135

Auvray, M. and Bey, I.: A modeling study of the background ozone over Europe: Origin and interannual variability, J. Geophys. Res., 110, D11303, doi:10.1029/2004JD005503, 2005. 6129, 6130, 6136

Baltensperger, U., Gaeggeler, H. W., Jost, D. T., Lugauer, M., Schikowski, M., Weingartenr, E., and Seibert, P.: Aerosol climatology at the high-alpine site Jungfraujoch, Switzerland, J. Geophys. Res., 102, 19 707–19 715, 1997. 6133, 6134

Bey, I., Jacob, D. J., Logan, J. A., and Yantosca, R. M.: Global modeling of tropospheric chemistry with assimilated meteorology: Model description and evaluation, J. Geophys. Res., 106, 23 073–23 095, 2001. 6134, 6135, 6136

Burrows, J., Dehn, A., Deters, B., Himmelmann, S., Richter, A., Voigt, S., and Orphal, J.: Atmospheric remote-sensing reference data from GOME: Part 1. Temperature-dependent absorption cross-sections of NO2 in the 231–794 nm range, J. Quant. Spectrosc. Rad. Transfer, 60, 1025–1031, 1998. 6132

Burrows, J. P., Weber, M., Buchwitz, M., Rozanov, V., Ladstätter-Weibenmayer, A., Richter, A., Debeek, R., Hoogen, R., Bramstedt, K., Eichmann, K.-U., Eisinger, M., and Perner, D.: The Global Ozone Monitoring Experiment (GOME): Mission concept and first results, J. Atmos. Sciences, 56, 151–175, 1999. 6132

Chin, M., Ginoux, P., Kinne, S., Torres, O., Holben, B., Duncan, B., Martin, R., Logan, J., Higurashi, A., and Nakajima, T.: Tropospheric aerosol optical thickness from GOCART model and comparisons with satellite and sunphotometer measurements, J. Atmos. Sci., 59, 461–483, 2002. 6135

Choi, Y., Wang, Y., Zeng, T., Martin, R. V., Kurosu, T. P., and Chance, K.: Evidence of lightning NO_x and convective transport of pollutants in satellite observations over North America, Geophys. Res. Lett., 32, doi:10.1029/2004GL021436, 2005. 6130

Cooper, O. R., Forster, C., Parrish, D., Trainer, M., Dunlea, E., Ryerson, T., Hübler, G., Nicks, D., Fehsenfeld, F., Holloway, J., de Gouw, J., Warneke, C., Roberts, J. M., Flocke, F., and Moody, J.: A case study of transpacific warm conveyor belt transport: Influence of merging airstreams on trace gas import to North America, J. Geophys. Res., 109, doi:10.1029/2003JD003624, 2004. 6138

Deeter, M. N., Emmons, L. K., Francis, G. L., Edwards, D. P., Gille, J. C., Warner, J. X., Khattatov, B., Ziskin, D., Lamarque, J.-F., Ho, S.-P., Yudin, V., Attié, J.-L., Packman, D., Chen, J., Mao, D., and Drummond, J. R.: Operational carbon monoxide retrieval algorithm and selected results for the MOPITT instrument, J. Geophys. Res., 108(D14), 4399,

doi:10.1029/2003JD003186, 2003. 6131
Duncan, B. and Bey, I.: A modeling study of export pathways of pollution from Europe: Seasonal and interannual variations., J. Geophys. Res., 109, D08301, doi:10.1029/2003JD004079, 2004. 6136
Duncan, B., Martin, R. V., Staudt, A. C., Yevich, R., and Logan, J. A.: Interannual and seasonnal variability of biomass burning emissions constrained by satellite observations, J. Geophys. Res., 108(D2), 4040, doi:10.1029/2002JD002378, 2003. 6135
Edwards, D. P., Halvorson, C., and Gille, J.: Radiative transfer modeling for the EOS Terra satellite Measurement of Pollution in the Troposphere (MOPITT) instrument, J. Geophys. Res., 104, 16 755–16 776, doi:10.1029/1999JD900167, 1999. 6131
Fiore, A., Jacob, D., Liu, H., Yantosca, R., Fairlie, T., and Li, Q.: Variability in surface ozone background over the United States: Implications for air quality policy, J. Geophys. Res., 108, 4787, doi:10.1029/2003JD003855, 2003. 6134
Fiore, A. M., Jacob, D., Bey, I., Yantosca, R., Field, B., Fusco, A., and Wilkinson, J.: Background ozone over the United States in summer: origin,trend, and contribution to pollution episodes, J. Geophys. Res., 107(D15), 4275, doi:10.1029/2001JD000982, 2002. 6136
Fusco, A. C. and Logan, J. A.: Analysis of 1970-1995 trends in tropospheric ozone at Northern Hemisphere midlatitudes with the GEOS-CHEM model, J. Geophys. Res., D108, doi:10.1029/2002JD002742, 2003. 6136
Heald, C., Jacob, D., Fiore, A., Emmons, L., Gille, J., Deeter, M., Warner, J., Edwards, D., Crawford, J., Hamlin, A., Sachse, G., Browell, E., Avery, M., Vay, S., Westberg, D., Blake, D., Singh, H., Sandholm, S., Talbot, R., and Fuelberg, H.: Asian outflow and trans-Pacific transport of carbon monoxide and ozone pollution: An integrated satellite, aircraft, and model perspective, J. Geophys. Res., 108(D24), 4808, doi:10.1029/2003JD003507, 2003. 6132
Kurosu, T. P., Chance, K., and Spurr, R. J. D.: CRAG-cloud retrieval algorithm for ESA's global ozone monitoring experiment, ESA WPP-161, pp. 513–521, eur. Space Res. and Tech Cent., Noordwijk, Netherlands, 1999. 6133
Lelieveld, J., Dentener, F. J., Peters, W., and Krol, M. C.: On the role of hydroxyl radicals in the self-cleansing capacity of the troposphere, Atmos. Chem. Phys., 4, 2337–2344, 2004, SRef-ID: 1680-7324/acp/2004-4-2337. 6136
Li, Q., Jacob, D., Bey, I., Palmer, P., Duncan, B., Field, B., Martin, R., Fiore, A., Yantosca, R., Parrish, D., Simmonds, P., and Oltmans, S.: Transatlantic transport of pollution and its effects on surface ozone in Europe and North America, J. Geophys. Res., 107(D14), 4166,

doi:10.1029/2001JD001422, 2002. 6129, 6136
Li, Q., Jacob, D., Park, R., Wang, Y., Heald, C., Hudman, R., Yantosca, R., Martin, R., and Evans, M.: North American pollution outflow and the trapping of convectively lifted pollution by upper-level anticyclone, J. Geophys. Res., 110, doi:10.1029/2004JD005039, 2005a. 6129, 6130, 6136, 6138, 6139, 6140
Lin, H. and Rood, R.: Multidimensional flux form semi-Lagrangian transport schemes, Mon. Weather Rev., 124, 2046–2070, 1996. 6135
Liu, H., Jacob, D., Bey, I., and Yantosca, R.: Constraints from 210Pb and 7Be on wet deposition and transport in a global three-dimensional chemical tracer model driven by assimilated meteorological fields, J. Geophys. Res., 106, 12 109–12 128, 2001. 6135
Martin, R. V., Chance, K., Jacob, D. J., Kurosu, T. P., Spurr, R. J. D., Bucsela, E., Gleason, J. F., Palmer, P. I., Bey, I., Fiore, A. M., Li, Q., Yantosca, R. M., and Koelemeijer, R. B. A.: An improved retrieval of tropospheric nitrogen dioxide from GOME, J. Geophys. Res., 107(D20), 4437, doi:10.1029/2001JD001027, 2002. 6132
Martin, R. V., Jacob, D., Yantosca, R., Chin, M., and Ginoux, P.: Global and Regional Decreases in Tropospheric Oxidants from Photochemical Effects of Aerosols, J. Geophys. Res., 108(D3), 4097, doi:10.1029/2002JD002622, 2003. 6132, 6134, 6135, 6136
Palmer, P. I., Jacob, D., Chance, K., Martin, R., Spurr, R., Kurosu, T., Bey, I., Yantosca, R., Fiore, A., and Li, Q.: Air mass factor formulation for spectroscopic measurements from satellites: Application to formaldehyde retrievals from the Global Ozone Monitoring Experiment, J. Geophys. Res., 106, 14 539–14 550, 2001. 6133
Park, R., Jacob, D. J., Field, B. D., Yantosca, R. M., and Chin, M.: Natural and transboundary pollution influences on sulfate-nitrate-ammonium aerosols in the United States: Implications for policy, J. Geophys. Res., 109, doi:10.1029/2003JD004473, 2004. 6134
Richter, A. and Burrows, J.: Tropospheric NO2 from GOME measurements, Adv. Space Res., 29, 1673–1683, 2002. 6132
Spivakovsky, C., Logan, J. A., Montzka, S. A., Balkanski, Y. J., Foreman-Fowler, M., Jones, D. B. A., Horowitz, L. W., Fusco, A. C., Brenninkmeijer, C. A. M., Prather, M. J., Wofsy, S. C., and McElroy, M. B.: Three-dimensional climatological distribution of tropospheric OH: Update and evaluation, J. Geophys. Res., 105, 8931–8980, 2000. 6136
Spurr, R. J. D.: Simultaneous derivation of intensities and weighting functions in a general pseudo-spherical discrete ordinate radiative transfer treatment, J. Quant. Spectrosc. Radiat. Transfer, 75, 129–175, 2002. 6133

Stohl, A.: A 1-year Lagrangian climatology of airstreams in the Northern Hemisphere troposphere and lowermost stratosphere, J. Geophys. Res., 106(D7), 7263–7280, 2001. 6130
Stohl, A. and Trickl, T.: A textbook example of long-range transport: Simultaneous observation of ozone maxima of stratospheric and North American origin in the free troposphere over Europe, J. Geophys. Res., 104, 30 445–30 462, 1999. 6129
Stohl, A., Eckhardt, S., Forster, C., James, P., and Spichtinger, N.: On the pathways and timescales of intercontinental air pollution transport, J. Geophys. Res., 107(D23), 4684, doi:10.1029/2001JD001396, 2002. 6129
Thouret, V., Marenco, A., Logan, J., Nédélec, P., and Grouhel, C.: Comparisons of ozone measurements from the MOZAIC airborne program and the ozone sounding network at eight locations, J. Geophys. Res., 103(D19), 25 695–25 720, 1998. 6134
Wang, Y., Jacob, D., and Logan, J.: Global simulation of tropospheric ozone-NO_x-Hydrocarbon chemistry, J. Geophys. Res., 103, 10 713–10 768, 1998a. 6135
Wang, Y., Jacob, D., and Logan, J.: Global simulation of tropospheric O_3-NO_x-hydrocarbon chemistry 1. Model formulation, J. Geophys. Res., 103(D9), 10 713–10 726, 1998b. 6135
Wesely, M.: Parameterization of surfaceresistance to gaseous dry deposition in regional-scale numerical models, Atmos. Environ., 23, 1293–1304, 1989. 6135
Wild, O., Zhu, Q., and Prather, M.: Fast-J: Accurate simulation of in- and below-cloud photolysis in global chemical models, J. Atmos. Chem., 37, 245–282, 2000. 6135
Zellweger, C., Forrer, J., Hofer, P., Nyeki, S., Schwarzenbach, B., Weingarter, E., Ammann, M., and Baltensperger, U.: Partitioning of reactive nitrogen (NOy) and dependence on meteorological conditions in the free troposphere, Atmos. Chem. Phys., 3, 779–796, 2003, SRef-ID: 1680-7324/acp/2003-3-779. 6133

Table 1. Statistical quantities for CO and NO_2 calculated between monthly mean columns from GEOS-CHEM, MOPITT and GOME in summer 2000. The GEOS-CHEM CO column is transformed as described in Sect. 2.1.

	June 2000	July 2000	August 2000
MOPITT mean [molec cm^{-2}]	$1.6\ 10^{18}$	$1.4\ 10^{18}$	$1.4\ 10^{18}$
CO column bias [molec cm^{-2}]	$1.1\ 10^{17}$ (7%)	$3.0\ 10^{17}$ (21%)	$3.0\ 10^{17}$ (21%)
CO column std [molec cm^{-2}]	$1.2\ 10^{17}$	$2.3\ 10^{17}$	$3.1\ 10^{17}$
CO column corr. coeff. (r)	0.59	0.62	0.72
GOME mean [molec cm^{-2}]	$7.6\ 10^{14}$	$7.3\ 10^{14}$	$9.2\ 10^{14}$
NO_2 column bias [molec cm^{-2}]	$-2.4\ 10^{14}$ (−32%)	$-3.0\ 10^{14}$ (−42%)	$-3.5\ 10^{14}$ (−38%)
NO_2 column std [molec cm^{-2}]	$4.9\ 10^{14}$	$5.8\ 10^{14}$	$5.8\ 10^{14}$
NO_2 column corr. coeff. (r)	0.81	0.75	0.84

Table 2. Statistical quantities calculated between O_3 from GEOS-CHEM and MOZAIC for i) tropospheric column (surface to 300 hPa), ii) PBL (surface to 800 hPa) and iii) FT (800 to 300 hPa). The values were calculated using all the individual profiles at Paris, Brussels and Frankfurt in summer 2000.

	June 2000	July 2000	August 2000	summer 2000
	i) all levels: from surface to 300 hPa			
MOZAIC mean [ppb]	52.1	48.1	48.5	49.6
bias [ppb]	−2.1 (−4%)	−2.9 (−5%)	−2.0 (−4%)	−2.3 (−4%)
corr. coeff. (r)	0.66	0.71	0.71	0.69
	ii) all levels in PBL: from surface to 800 hPa			
MOZAIC PBL mean [ppb]	44.6	35.5	40.6	40.2
PBL bias [ppb]	0.9 (2%)	4.2 (12%)	2.0 (5%)	3.4 (6%)
PBL corr. coeff. (r)	0.64	0.54	0.69	0.62
	iii) all levels in FT: from 800 to 300 hPa			
MOZAIC FT mean [ppb]	60.6	61.9	57.2	59.9
FT bias [ppb]	−5.3 (−9%)	−9.70 (−16%)	−6.5 (−11%)	−7.2 (−12%)
FT corr. coeff. (r)	0.49	0.60	0.58	0.56

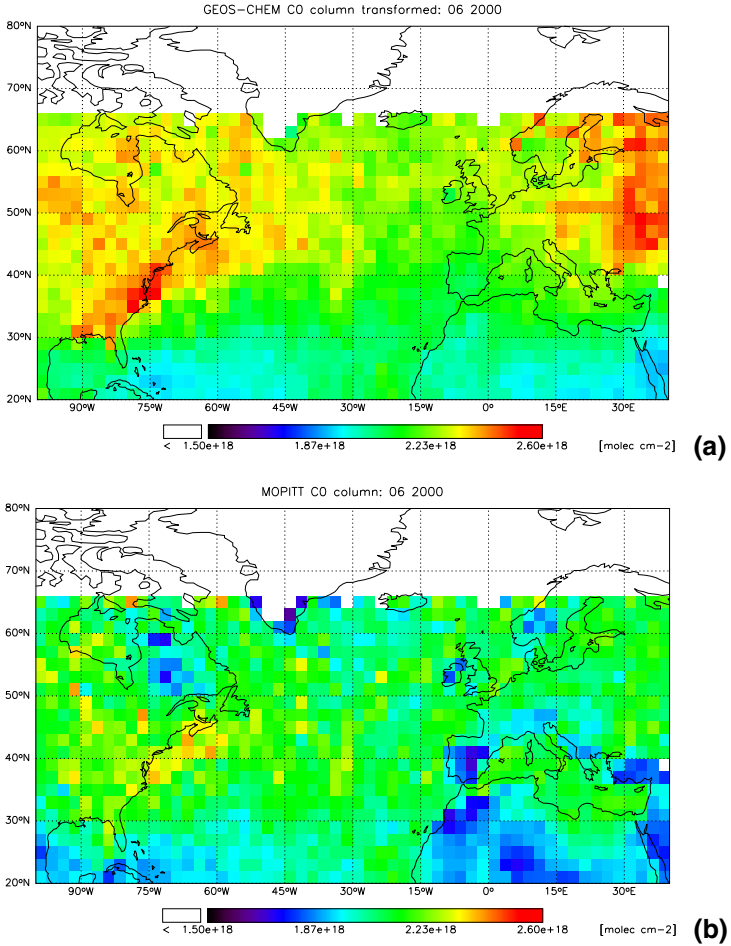

Fig. 1. Monthly mean CO column in June 2000 from: **(a)** GEOS-CHEM (transformed) and **(b)** MOPITT. **(c)** scatter plot GEOS-CHEM vs. MOPITT.

ACPD

5, 6127–6184, 2005

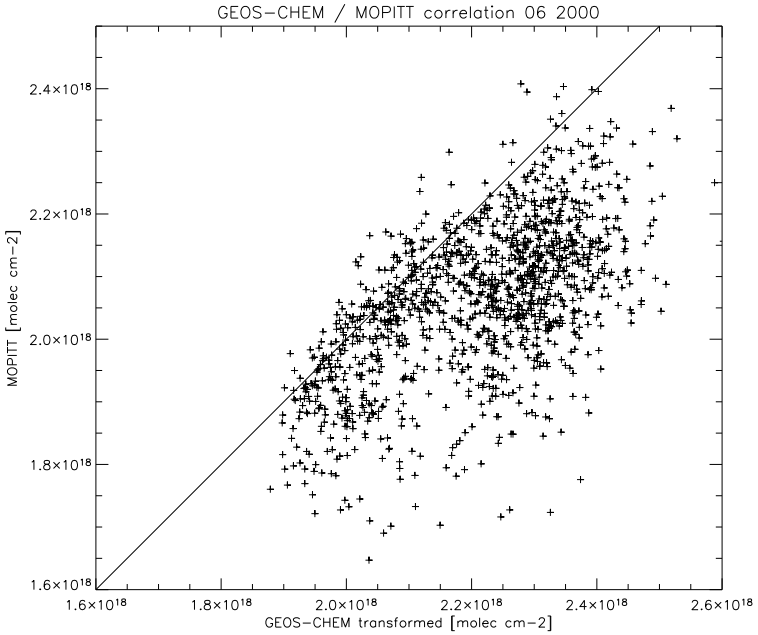

(c)

Fig. 1. Continued.

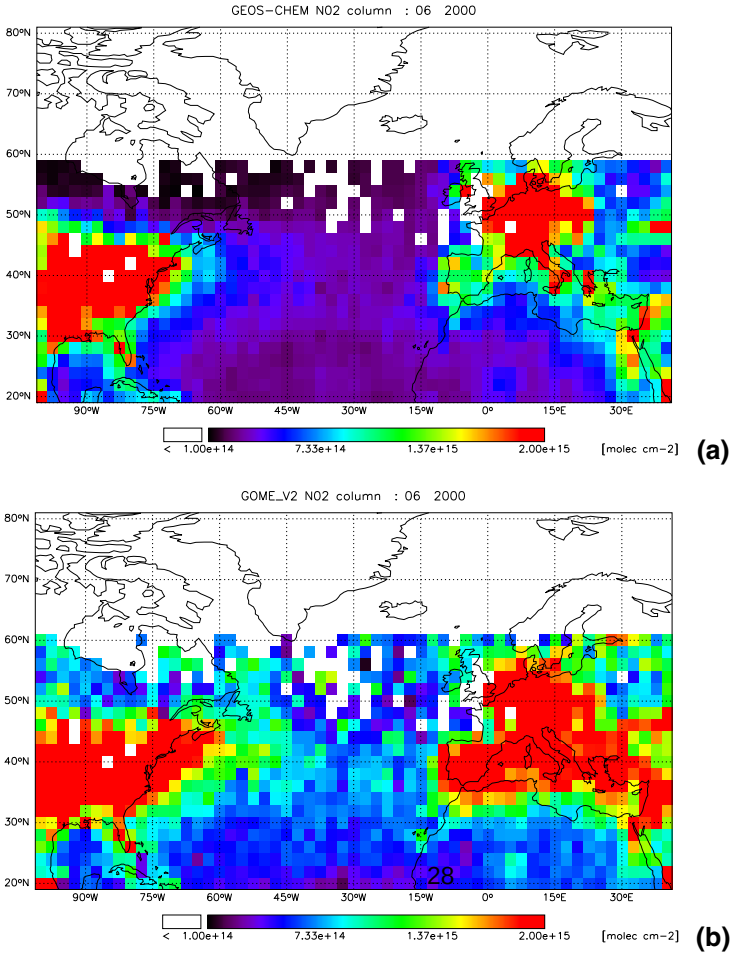

Fig. 2. Mean cloud-filtered tropospheric NO_2 columns in June 2000 from: **(a)** GEOS-CHEM and **(b)** GOME. **(c)** scatter plot GEOS-CHEM vs. GOME.

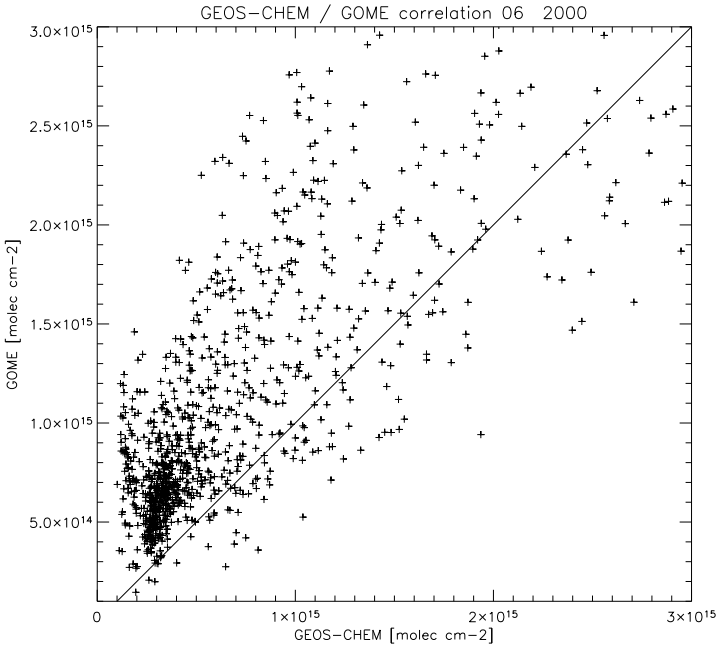

(c)

Fig. 2. Continued.

ACPD
5, 6127–6184, 2005

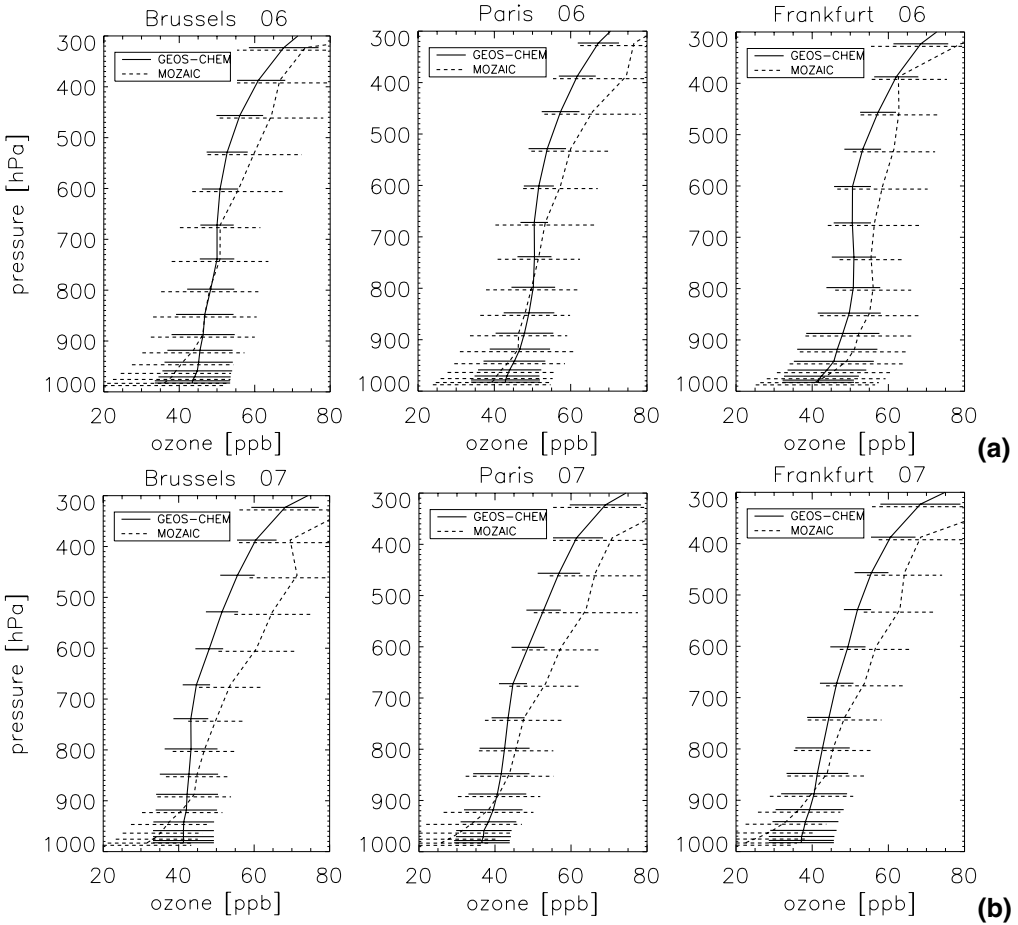

Fig. 3. Ozone monthly averaged and standard deviation from MOZAIC (dashed line) and GEOS-CHEM (solid line) at Brussels, Paris and Frankfurt in **(a)** June 2000, **(b)** July 2000 and **(c)** August 2000.

ACPD
5, 6127–6184, 2005

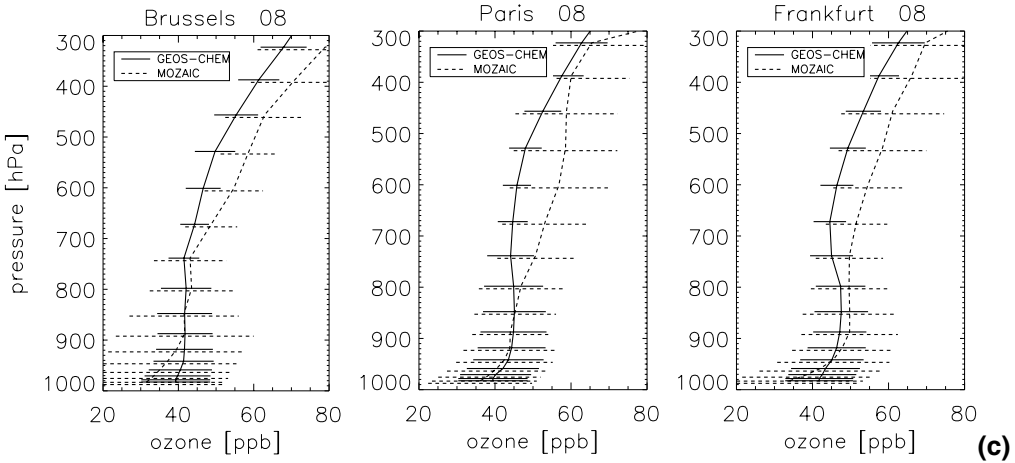

Fig. 3. Continued.

ACPD
5, 6127–6184, 2005

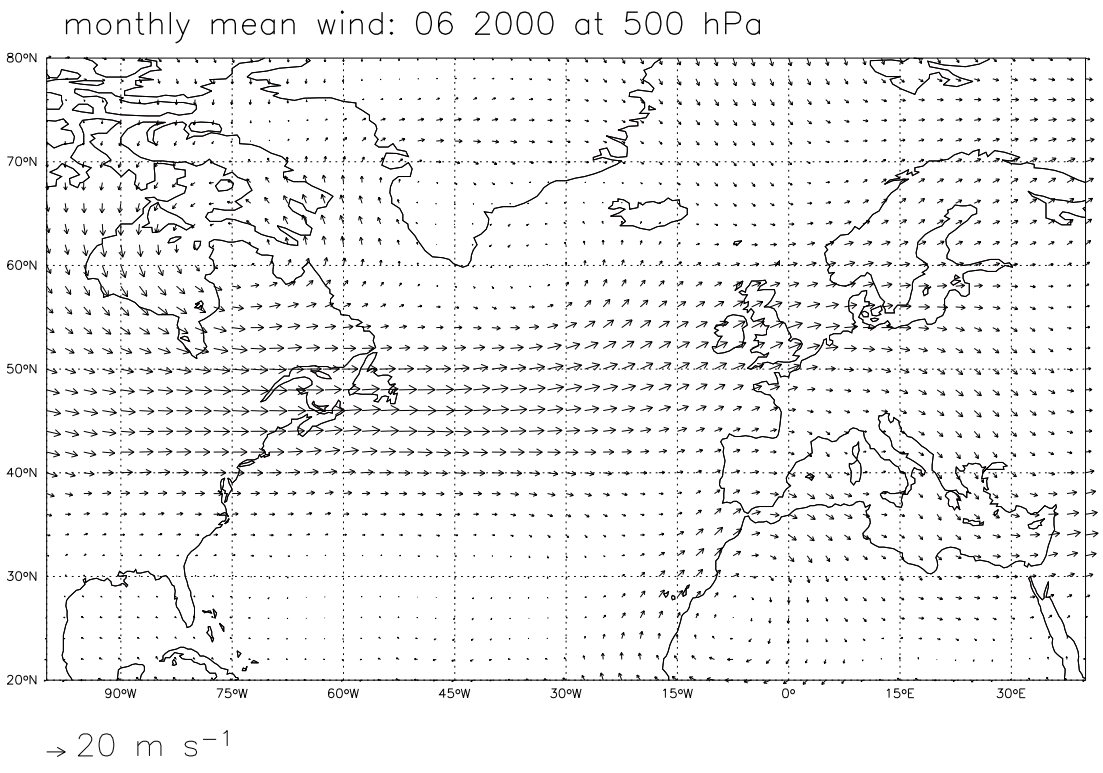

(a)

Fig. 4. GEOS-CHEM monthly mean winds at 500 hPa for: **(a)** June 2000, **(b)** July 2000, and **(c)** August 2000.

ACPD
5, 6127–6184, 2005

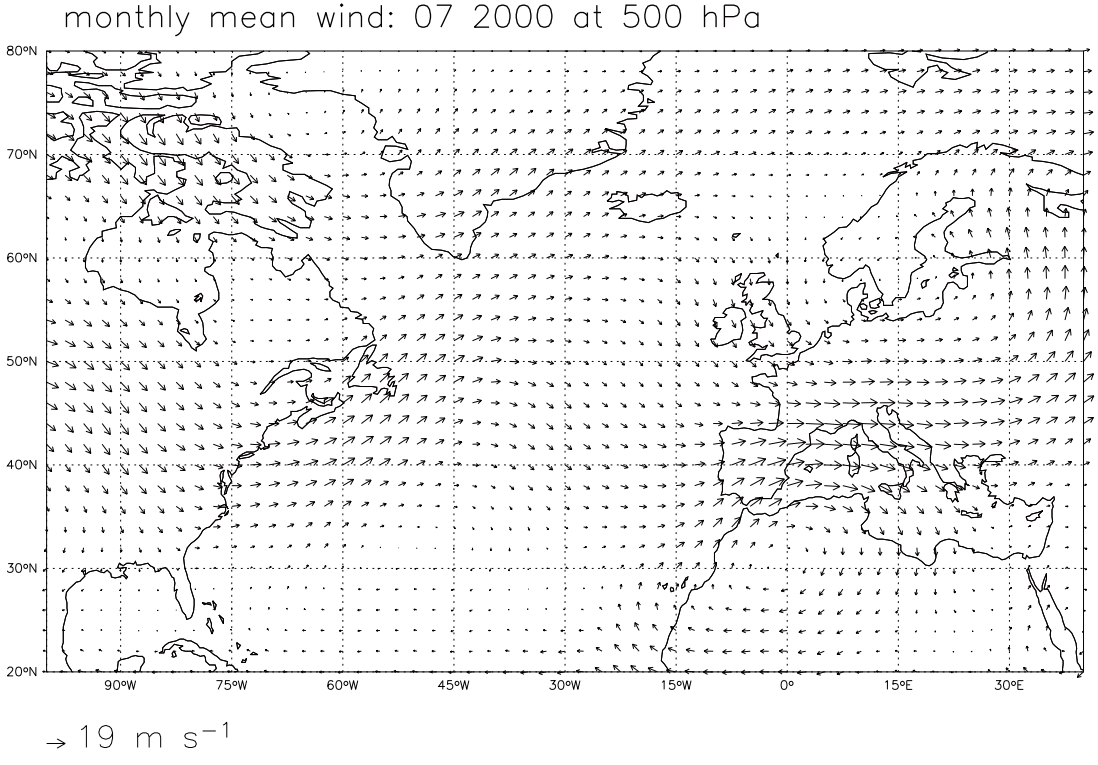

(b)

Fig. 4. Continued.

ACPD
5, 6127–6184, 2005

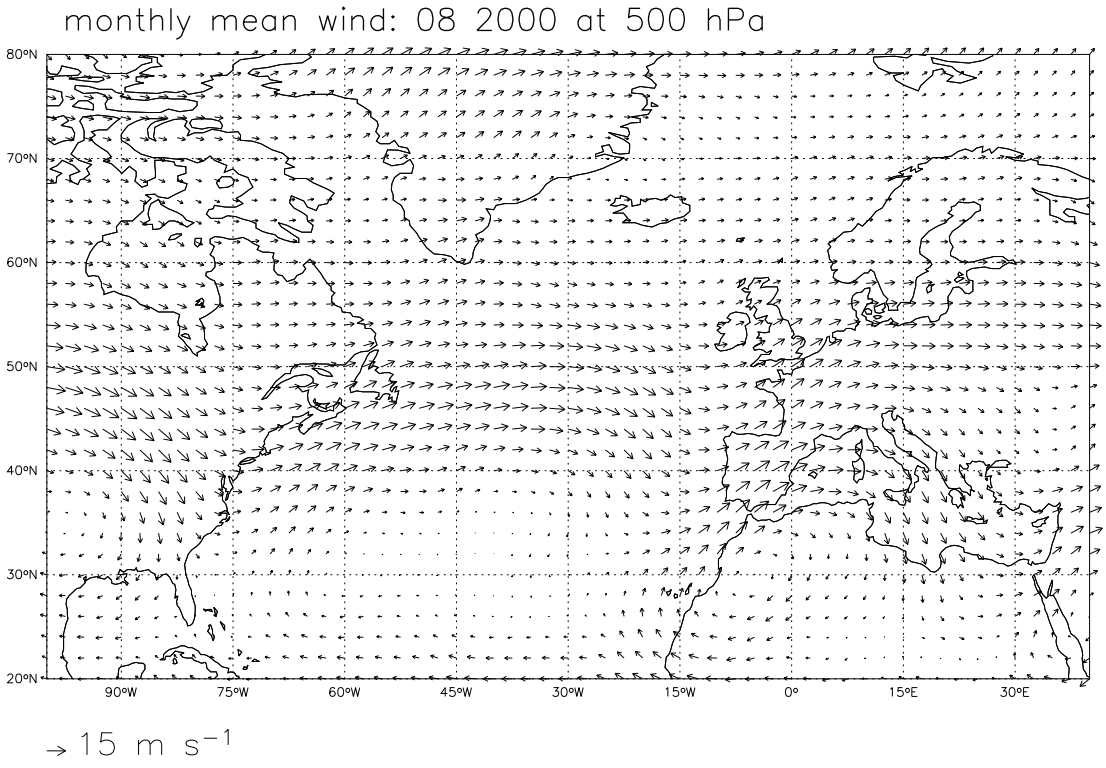

(c)

Fig. 4. Continued.

ACPD
5, 6127–6184, 2005

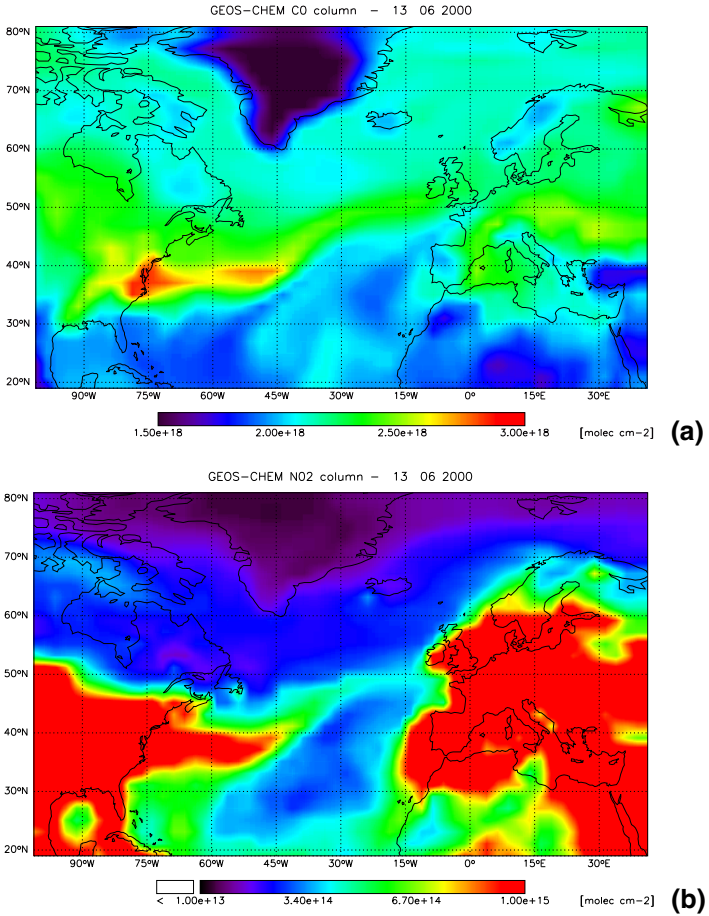

Fig. 5. Illustration of LRT1 event: **(a)** GEOS-CHEM CO column on 13 June, **(b)** GEOS-CHEM NO_2 column on 13 June, **(c)** MOPITT CO column for 9–13 June, **(d)** GOME NO_2 column on 11–13 June and **(e)** GEOS-CHEM mean sea level pressure and 500 hPa winds on 13 June.

ACPD
5, 6127–6184, 2005

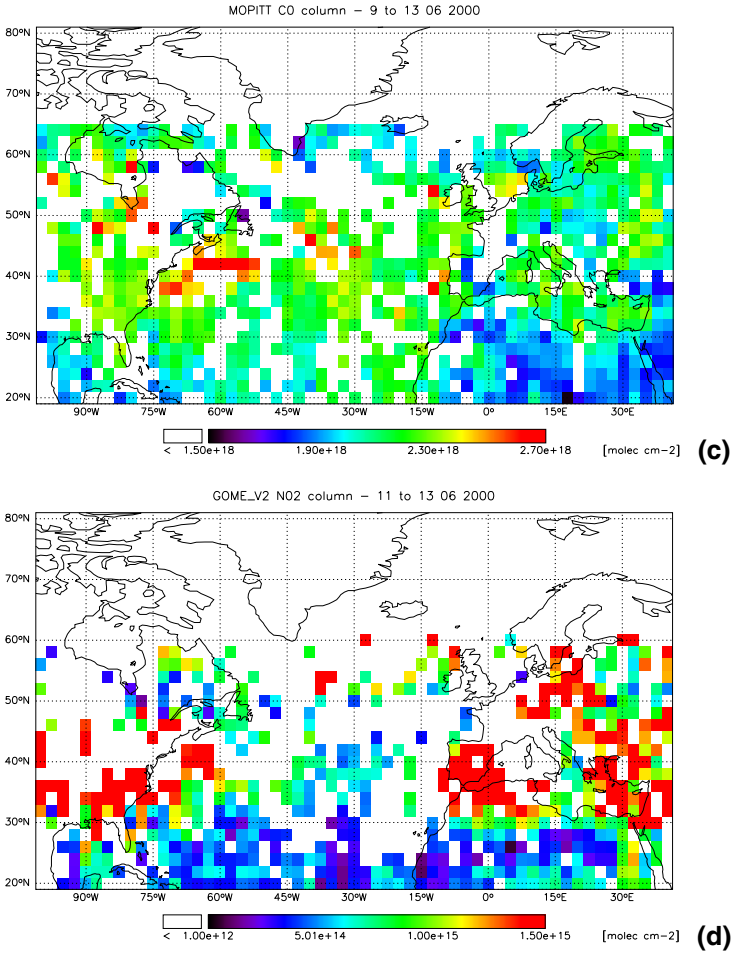

Fig. 5. Continued.

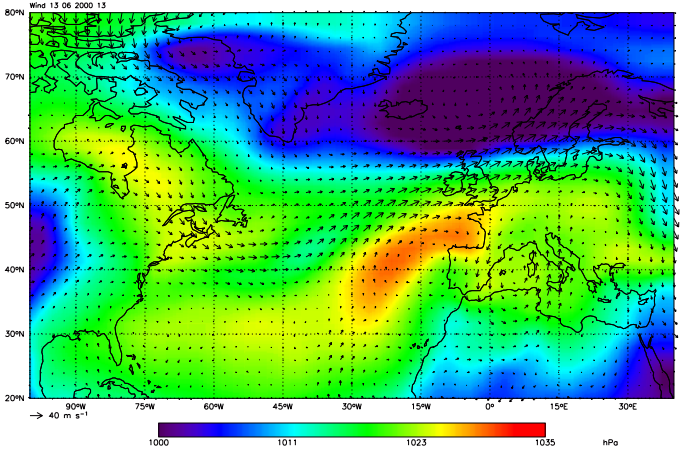

(e)

Fig. 5. Continued.

ACPD

5, 6127–6184, 2005

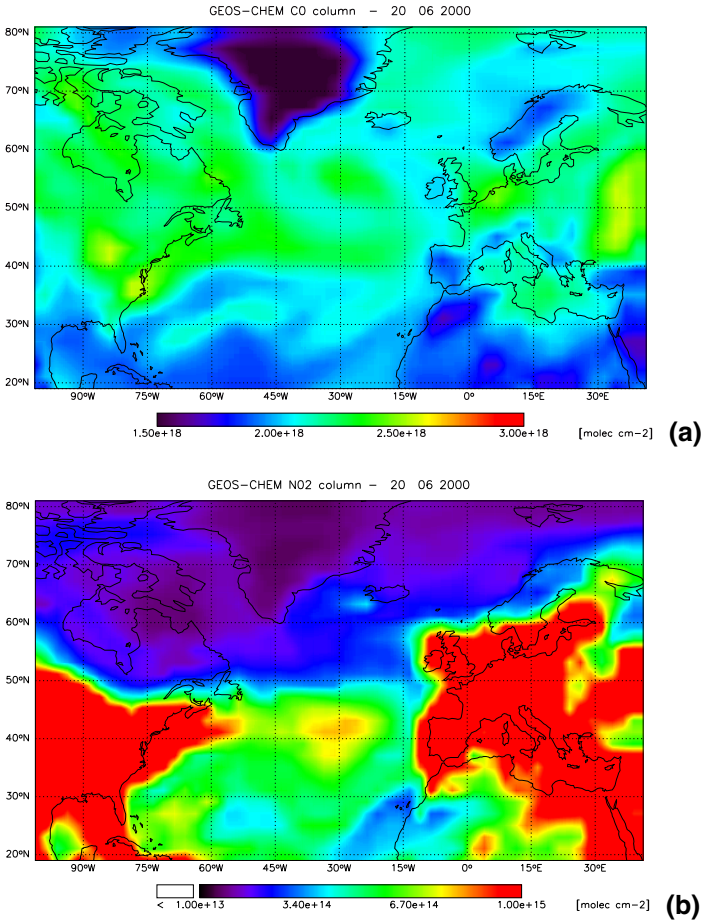

Fig. 6. Illustration of LRT2 event: **(a)** GEOS-CHEM CO column on 20 June, **(b)** GEOS-CHEM NO_2 column on 20 June, **(c)** MOPITT CO column for 19–21 June, **(d)** GOME NO_2 column for 19–21 June and **(e)** GEOS-CHEM mean sea level pressure and 500 hPa winds on 20 June.

ACPD
5, 6127–6184, 2005

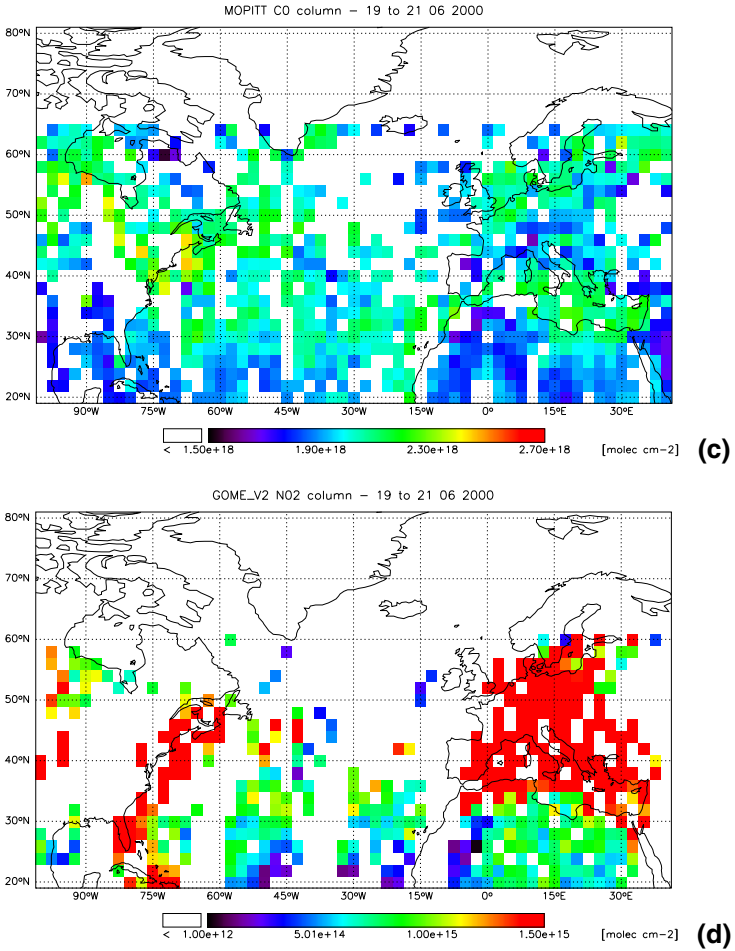

Fig. 6. Continued.

ACPD
5, 6127–6184, 2005

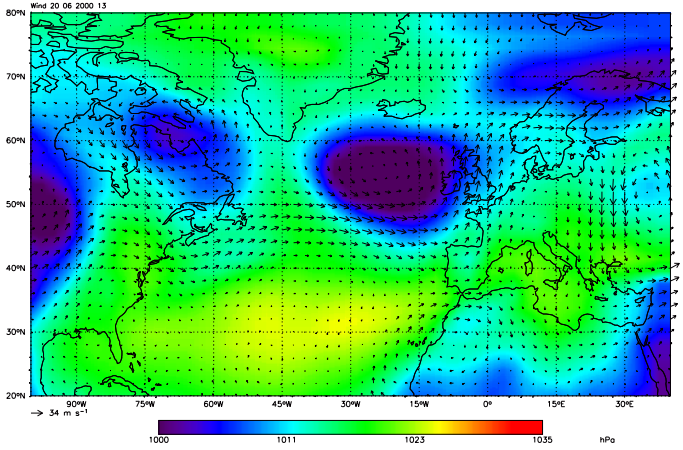

(e)

Fig. 6. Continued.

ACPD

5, 6127–6184, 2005

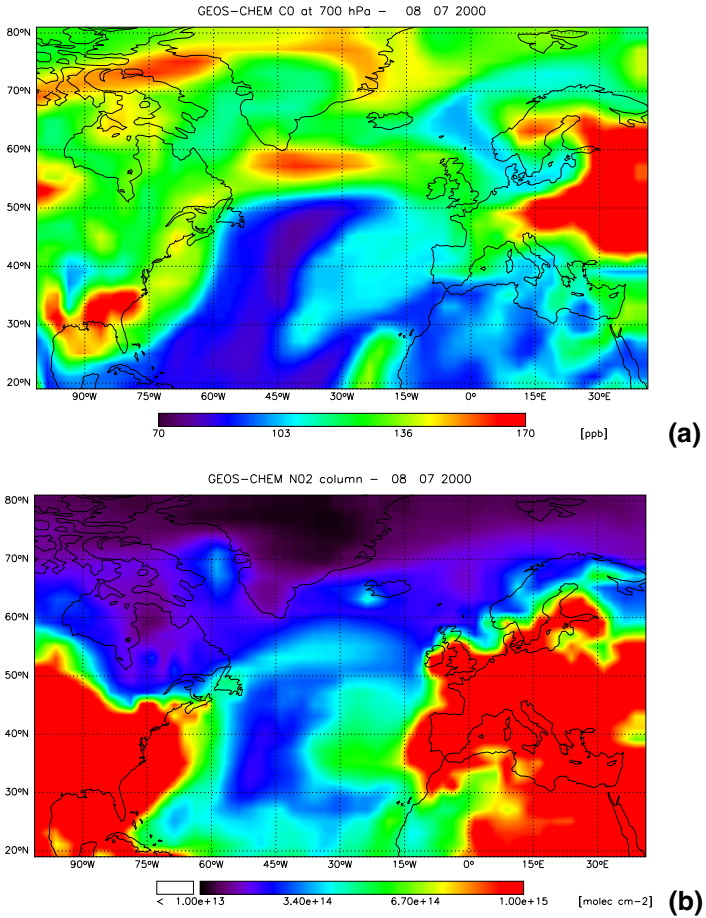

Fig. 7. Illustration of LRT4 event: **(a)** GEOS-CHEM CO at 700 hPa on 8 July, **(b)** GEOS-CHEM NO_2 column on 8 July, **(c)** GEOS-CHEM mean sea level pressure and 500 hPa winds on 8 July.

ACPD
5, 6127–6184, 2005

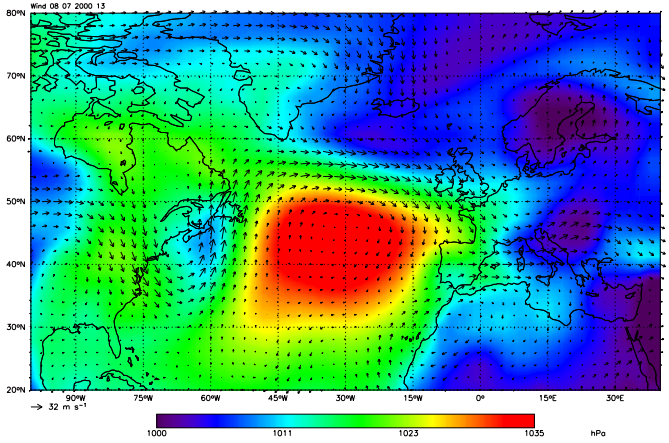

(c)

Fig. 7. Continued.

ACPD

5, 6127–6184, 2005

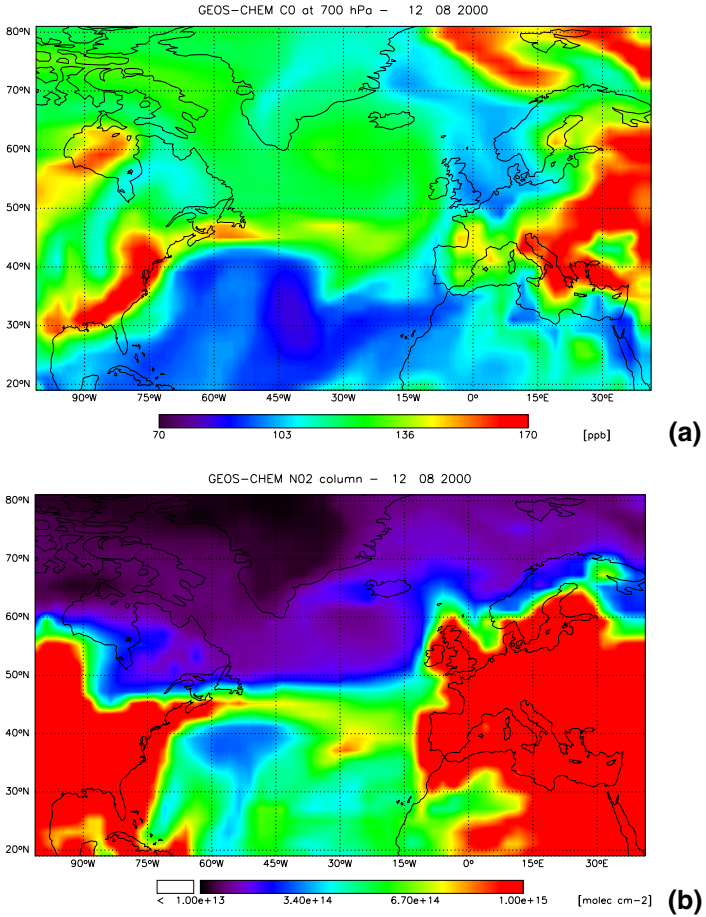

Fig. 8. Illustration of LRT9 event: **(a)** GEOS-CHEM CO at 700 hPa on 12 August, **(b)** GEOS-CHEM NO_2 column on 12 August, **(c)** MOPITT CO column from 10–14 August, **(d)** GOME v1 NO_2 column [molec cm^{-2}] from 10–14 August and **(e)** GEOS-CHEM mean sea level pressure and 500 hPa winds on 12 August.

ACPD
5, 6127–6184, 2005

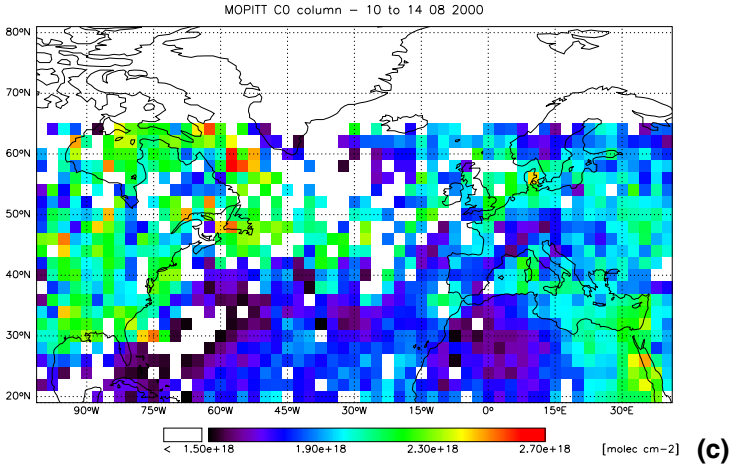

(c)

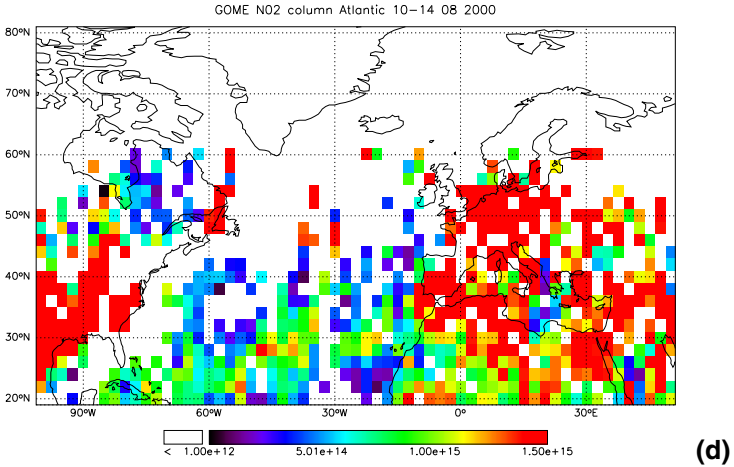

(d)

Fig. 8. Continued.

ACPD

5, 6127–6184, 2005

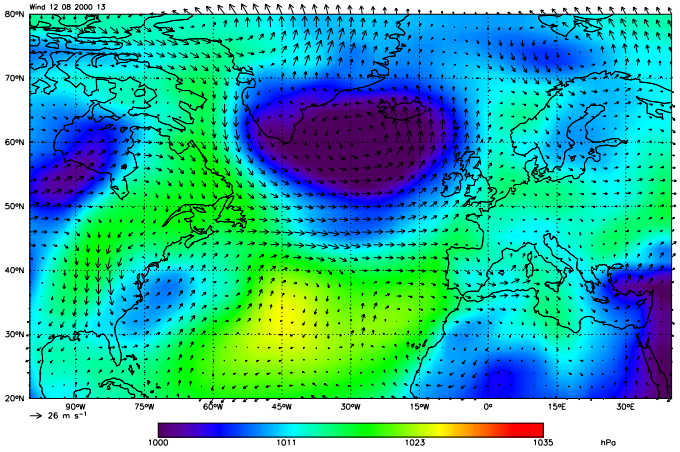

(e)

Fig. 8. Continued.

ACPD

5, 6127–6184, 2005

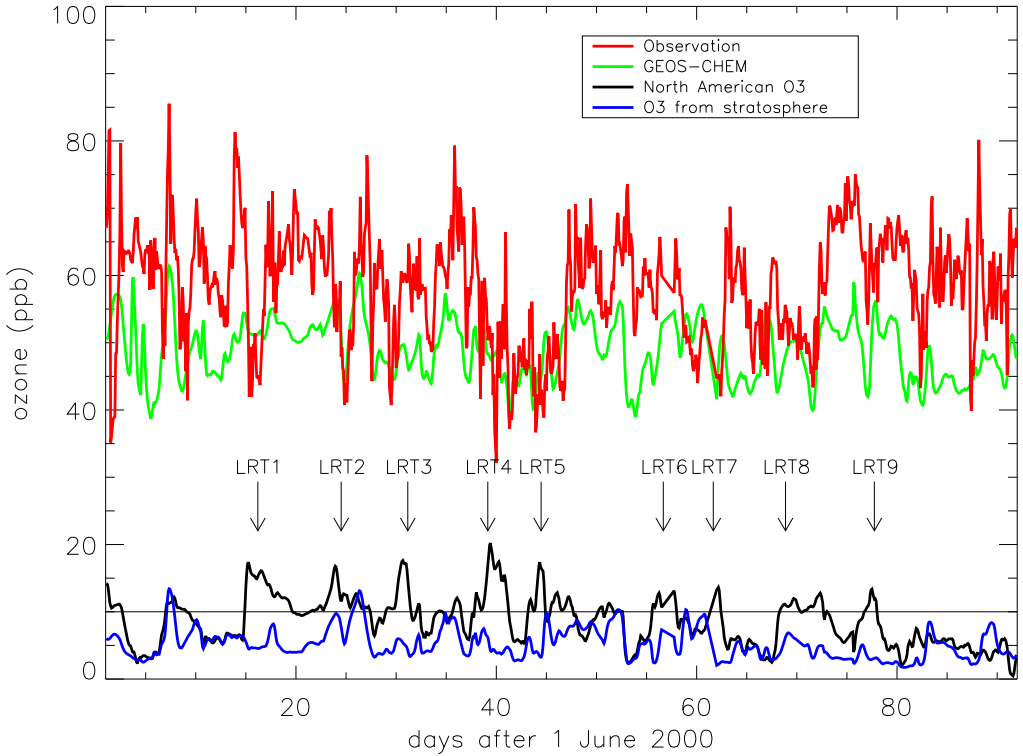

Fig. 9. Surface O_3 at JFJ in the period June–August 2000. Observed O_3 (red line), model total O_3 (green line), model North American O_3 (black line), and model stratospheric O_3 (blue line).

ACPD
5, 6127–6184, 2005

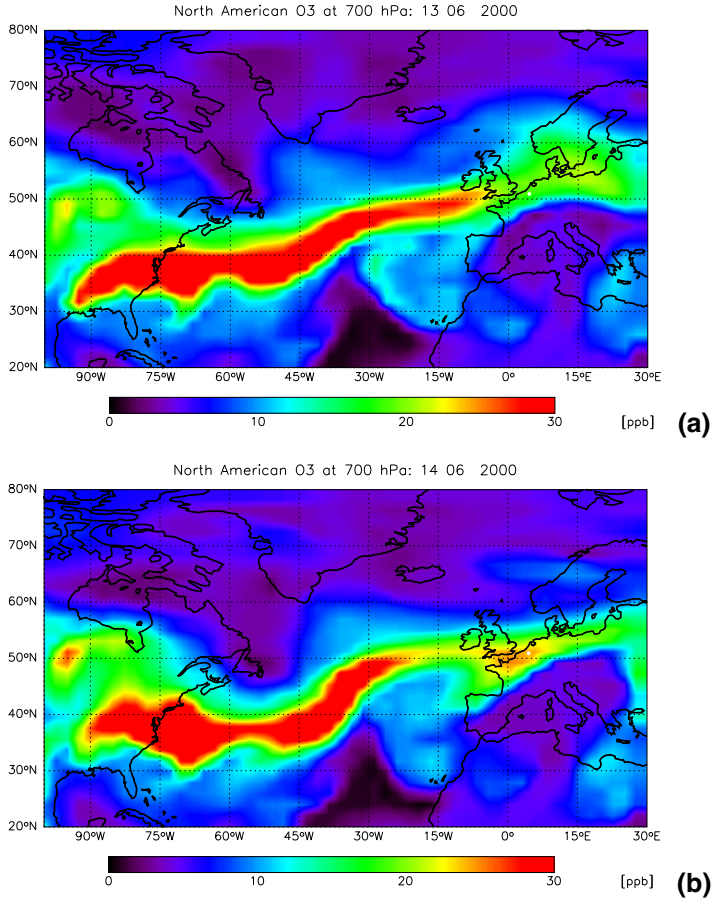

Fig. 10. LRT1 : **(a)** and **(b)** Daily averaged North American ozone at 700 hPa on 13 and 14 June. **(c)** O_3 mean and standard deviation for the period 13–15 June at Brussels from GEOS-CHEM (solid line) and MOZAIC (dashed line). **(d)** GEOS-CHEM profiles at Brussels 13–15 June, North American O_3 (dash-dotted line) and stratospheric O_3 (dashed line). **(e)** MOZAIC profiles at Brussels 13–15 June.

ACPD
5, 6127–6184, 2005

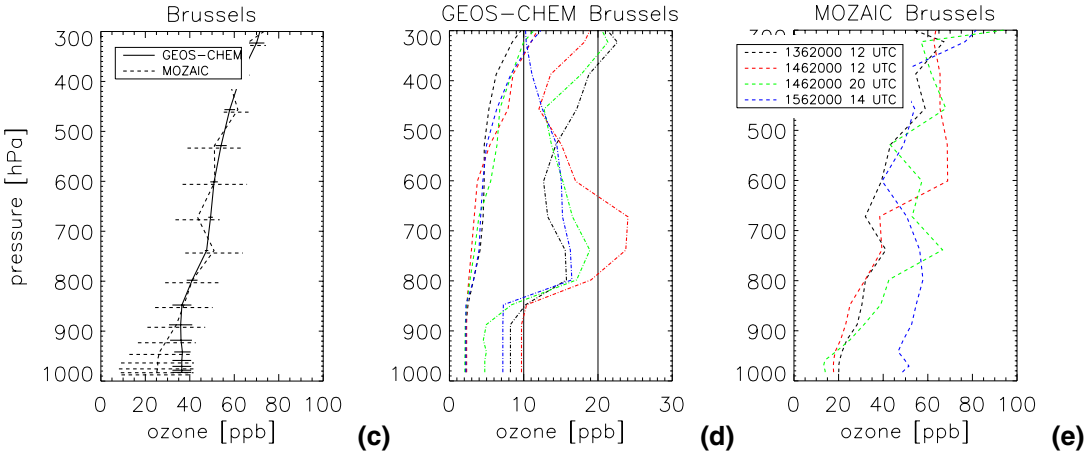

Fig. 10. Continued.

ACPD
5, 6127–6184, 2005

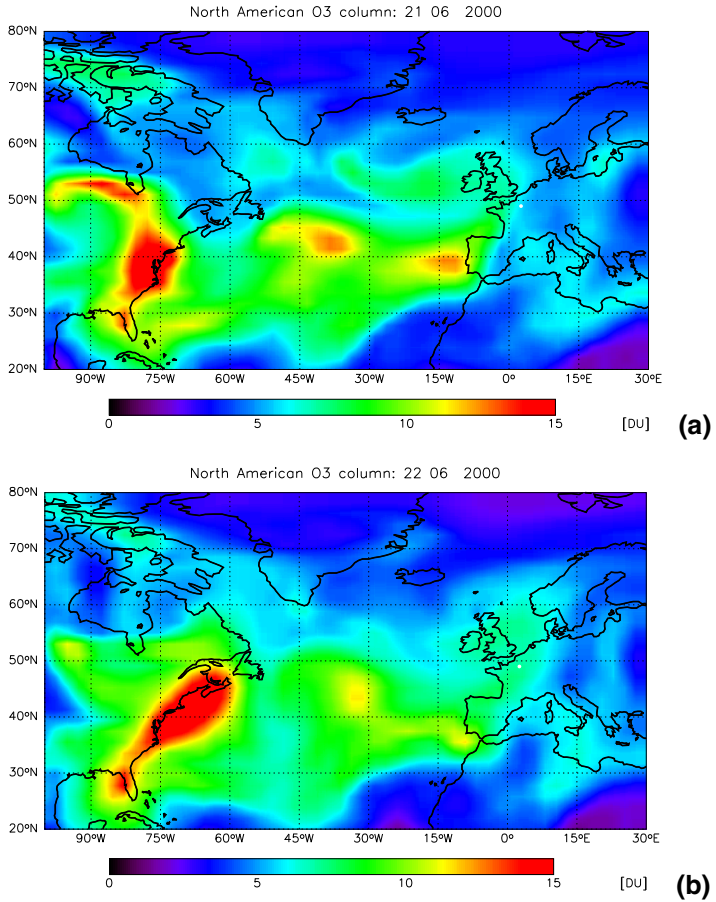

Fig. 11. LRT2 : **(a)** and **(b)** Daily averaged North American ozone column on 21 and 22 June. **(c)** O_3 mean and standard deviation for the period 21–23 June at Paris from GEOS-CHEM (solid line) and MOZAIC (dashed line). **(d)** GEOS-CHEM profiles at Paris on 21–23 June, North American O_3 (dash-dotted line) and stratospheric O_3 (dashed line). **(e)** MOZAIC profiles at Paris on 21–23 June.

ACPD
5, 6127–6184, 2005

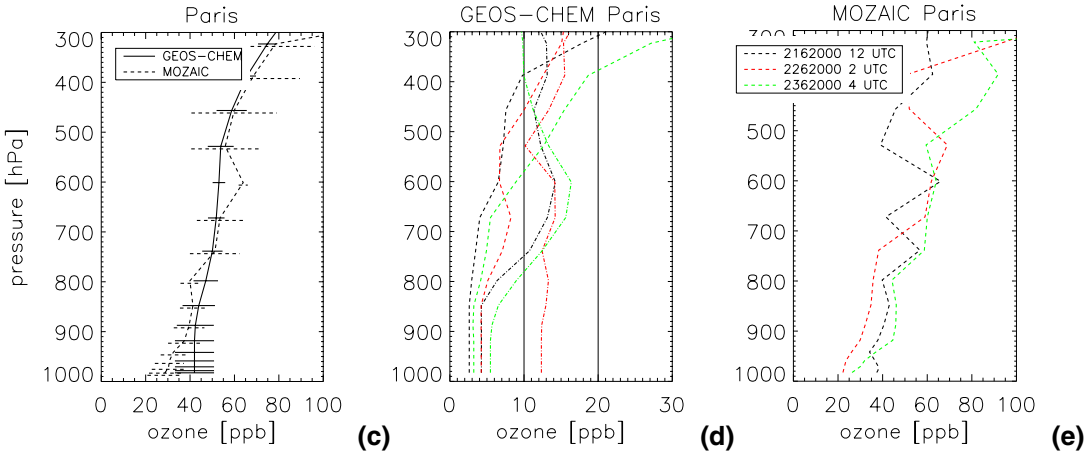

Fig. 11. Continued.

ACPD
5, 6127–6184, 2005

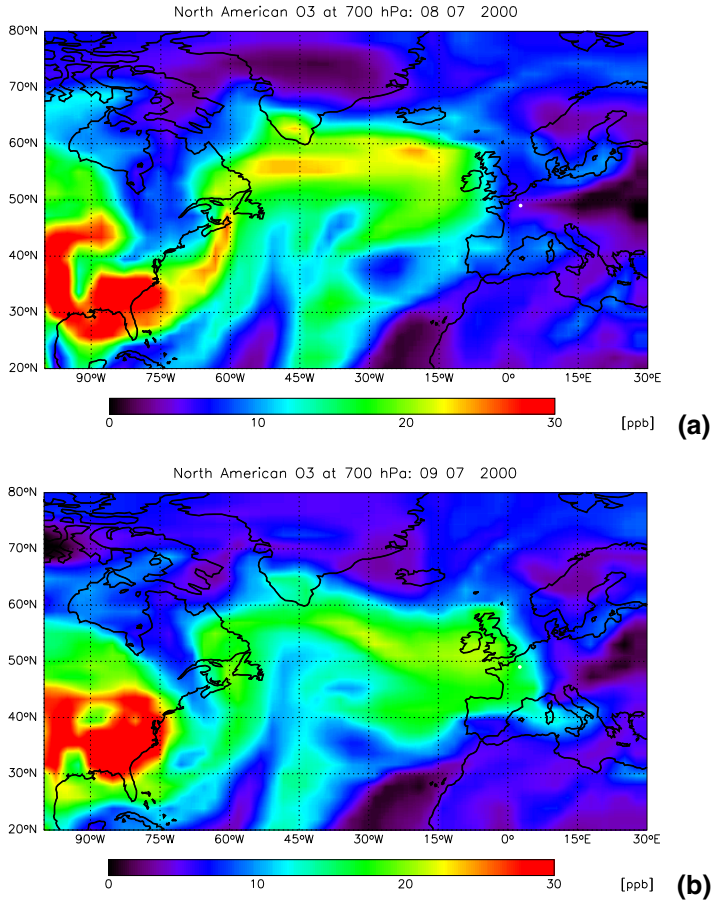

Fig. 12. LRT4 : Daily averaged North American ozone at 700 hPa on **(a)** 8 July and **(b)** 9 July 2000. **(c)** O_3 mean and standard deviation for the period 8–10 July at Paris from GEOS-CHEM (solid line) and MOZAIC (dashed line). **(d)** GEOS-CHEM profiles at Paris on 8–10 July, North American O_3 (dash-dotted line) and stratospheric O_3 (dashed line). **(e)** MOZAIC profiles at Paris on 8–10 July.

ACPD
5, 6127–6184, 2005

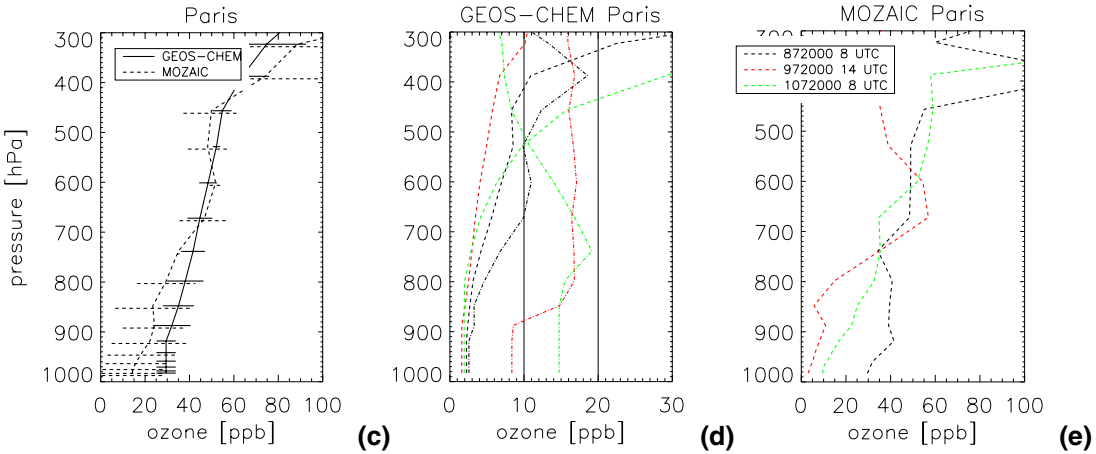

Fig. 12. Continued.

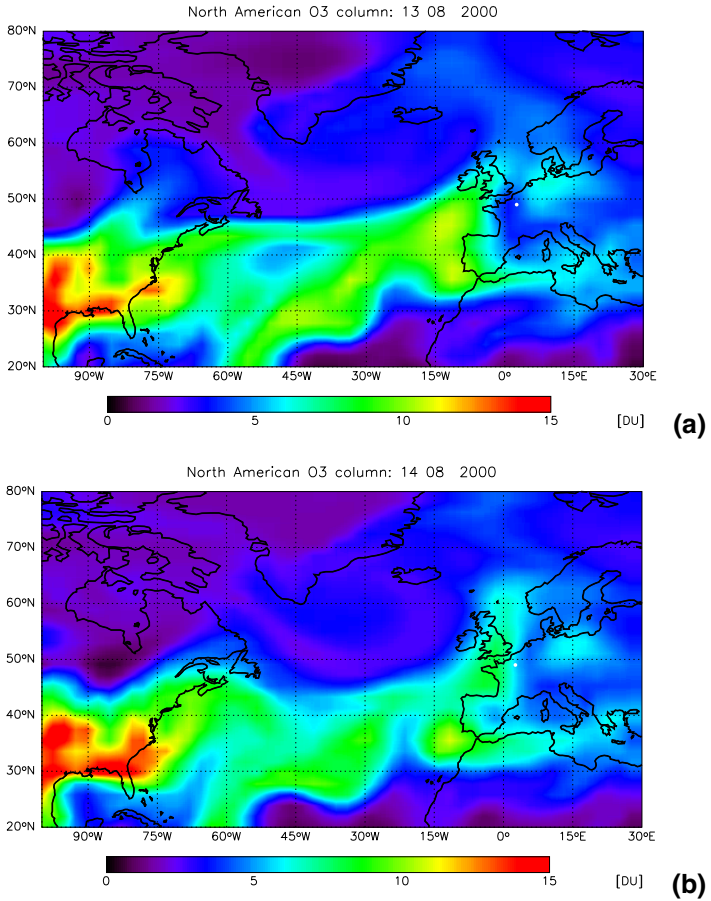

Fig. 13. LRT9 : North American ozone column on **(a)** 13 August and **(b)** 14 August 2000. **(c)** O_3 mean and standard deviation for the period 13–15 August at Paris from GEOS-CHEM (solid line) and MOZAIC (dashed line). **(d)** GEOS-CHEM profiles at Paris on 13–15 August, North American O_3 (dash-dotted line) and stratospheric O_3 (dashed line). **(e)** MOZAIC profiles at Paris on 13–15 August.

ACPD
5, 6127–6184, 2005

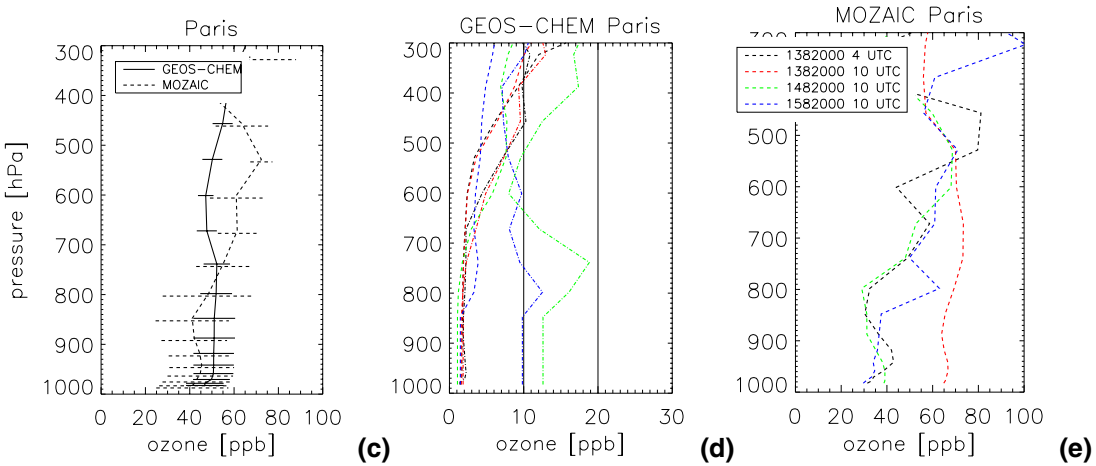

Fig. 13. Continued.

ACPD
5, 6127–6184, 2005

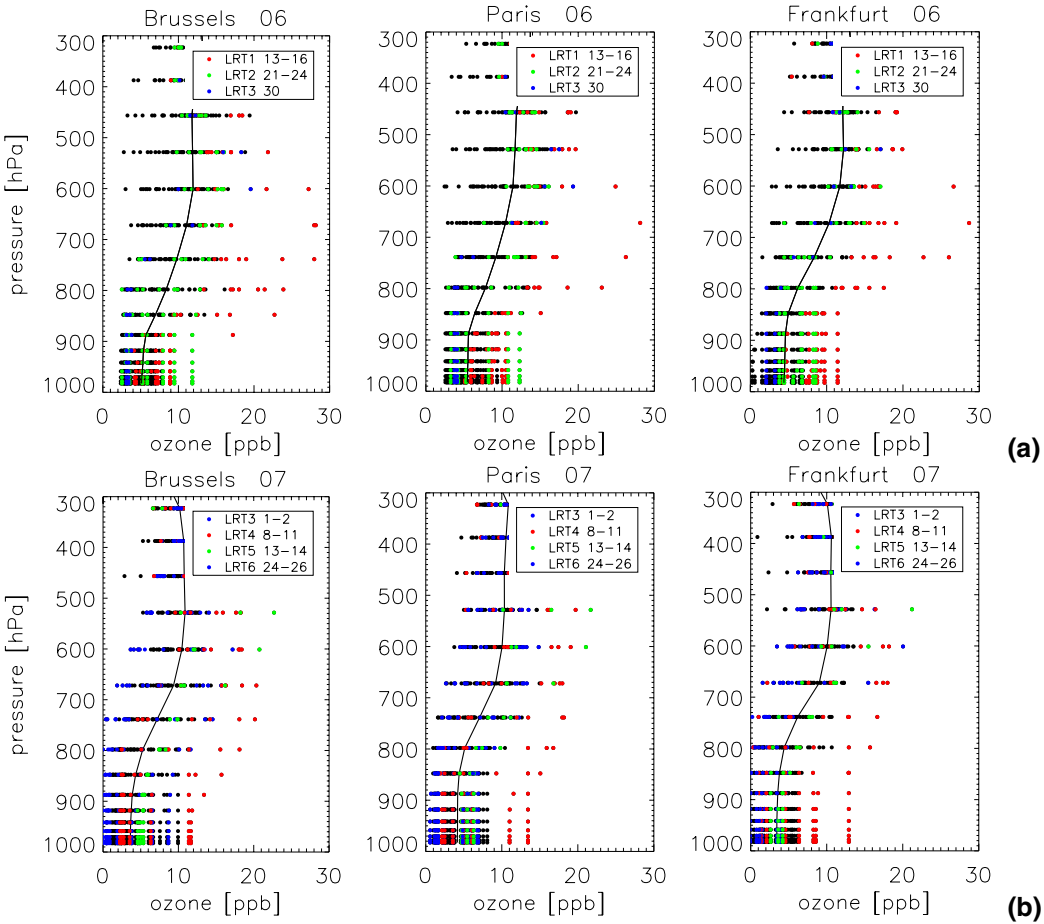

Fig. 14. North American O_3 contributions from GEOS-CHEM at Brussels, Paris and Frankfurt in **(a)** June 2000, **(b)** July 2000 and **(c)** August 2000. The solid line corresponds to the monthly averaged profile and the dots correspond to instantaneous contributions at 00:00 and 12:00 UTC for each day of the month.

ACPD
5, 6127–6184, 2005

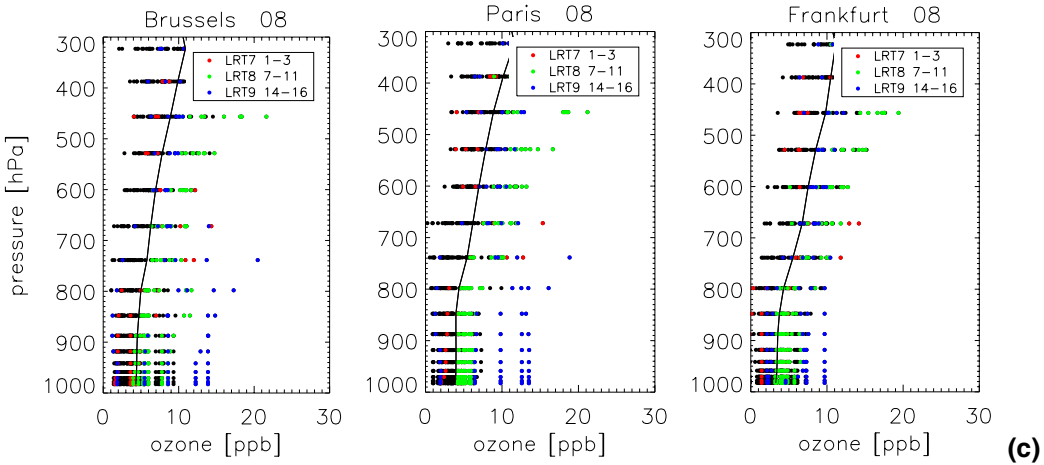

Fig. 14. Continued.

ACPD
5, 6127–6184, 2005